

# X-ray Photoelectron Spectroscopy (XPS)

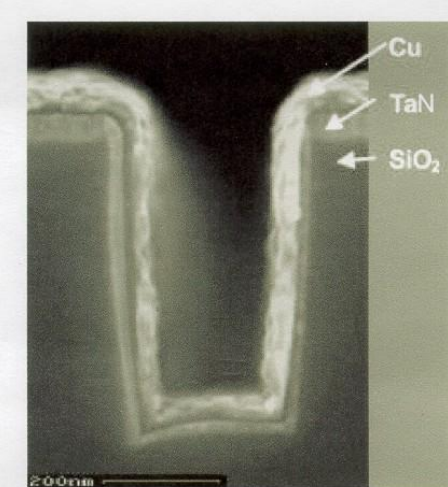
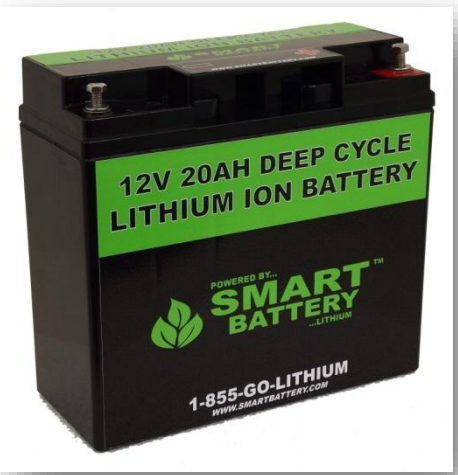
RICK HAASCH, PH.D.

UNIVERSITY OF ILLINOIS AT  
URBANA-CHAMPAIGN



Materials Research Laboratory  
GRAINGER COLLEGE OF ENGINEERING

# Surfaces and Interfaces







*“God made the bulk; the surface was invented by  
the devil.”*

— Wolfgang Pauli

# Particle Surface Interactions

Primary beam  
(source)

Ions

Electrons

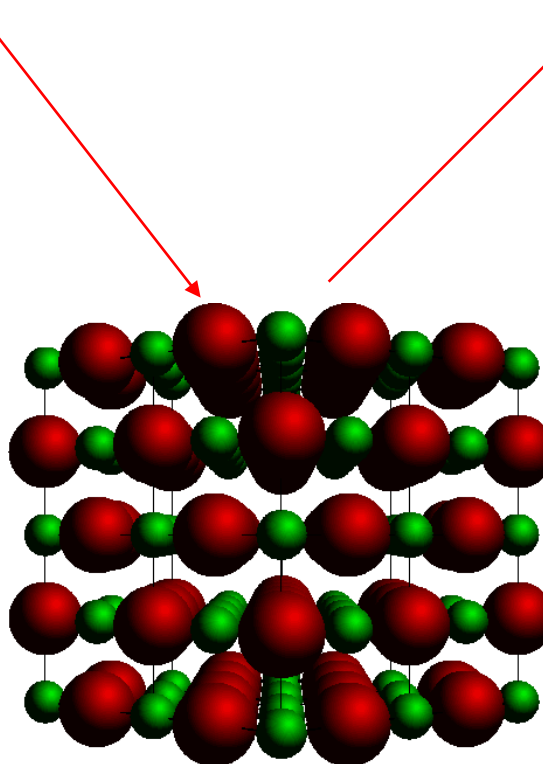
Photons

Secondary beam  
(spectrometers, detectors)

Ions

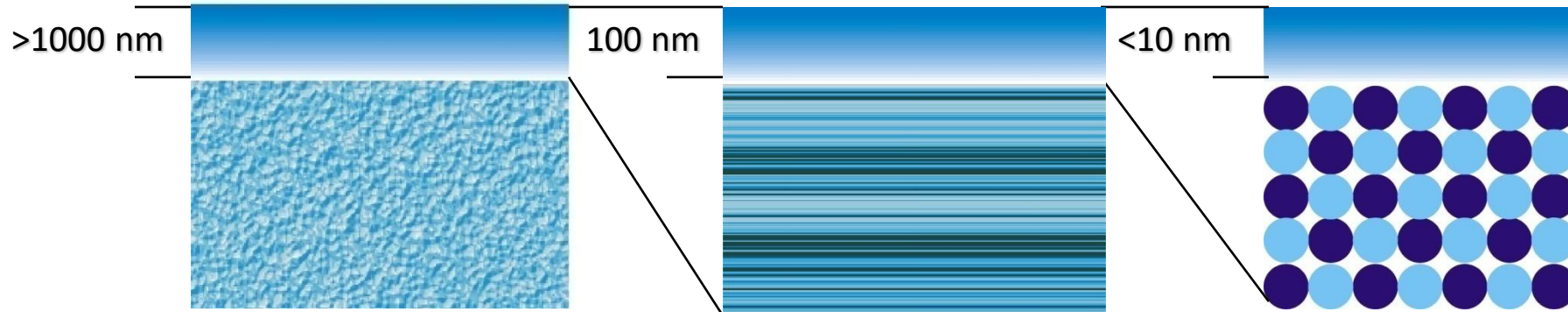
Electrons

Photons



I

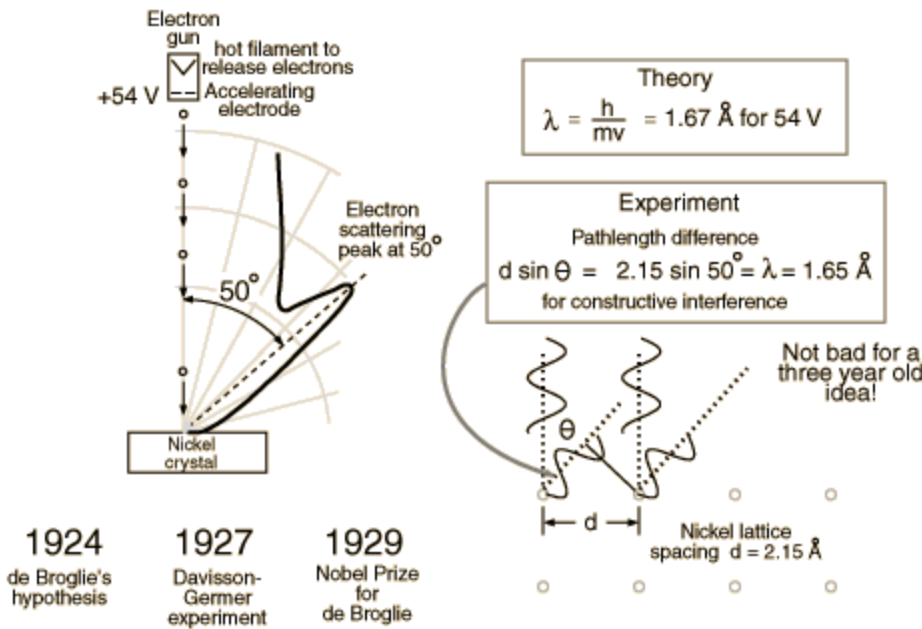
# What is the Surface?



Bulk Analysis

Thin-film Analysis

Surface Analysis

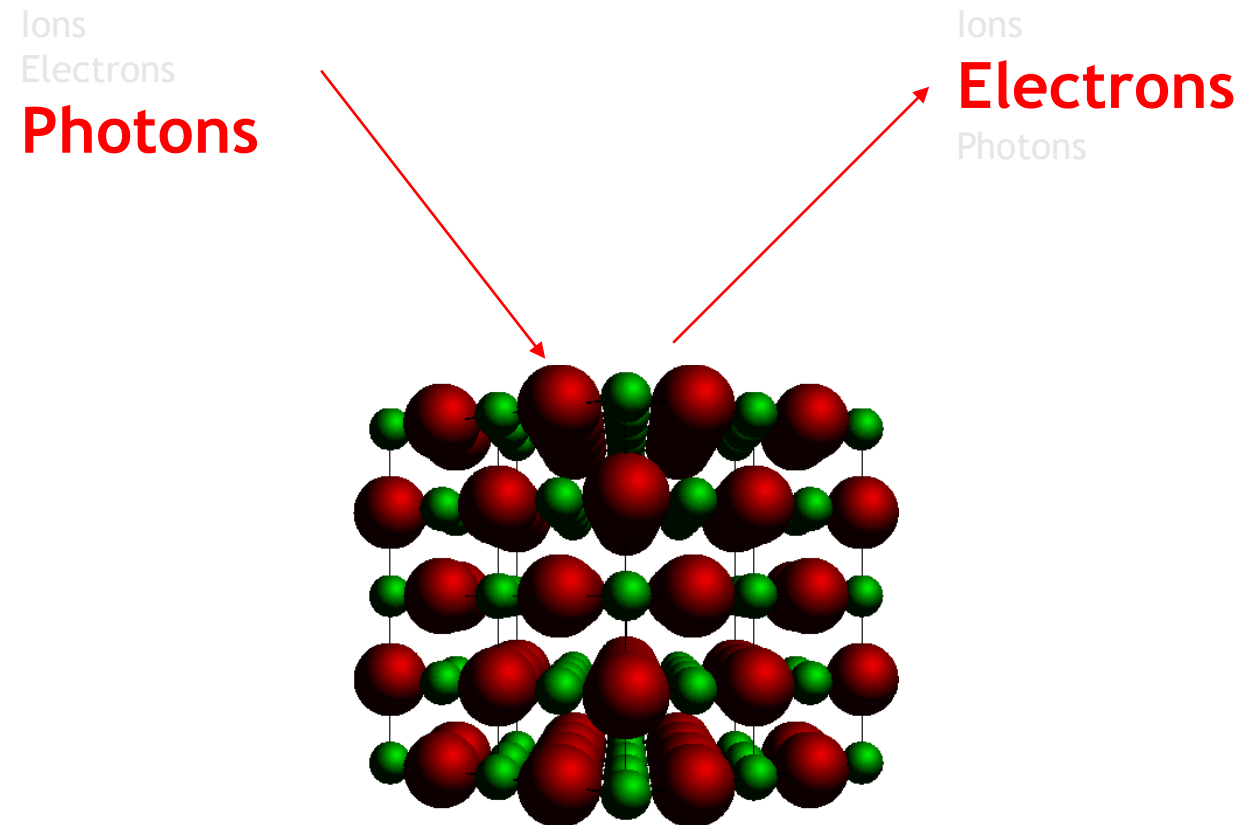


**For an electron** with KE = 1 eV and rest mass energy of 0.511 MeV, the de Broglie wavelength is **1.23 nm** (~1000X less than a 1 eV photon).

<http://hyperphysics.phy-astr.gsu.edu/hbase/davger.html#c1>

# Particle Surface Interactions

## Photoelectron Spectroscopy



I

Vacuum

© 2025 University of Illinois Board of Trustees. All rights reserved.

# X-ray Photoelectron Spectroscopy (XPS)

**X-ray Photoelectron Spectroscopy (XPS)**, also known as **Electron Spectroscopy for Chemical Analysis (ESCA)** is a widely used technique to investigate the chemical composition of surfaces.

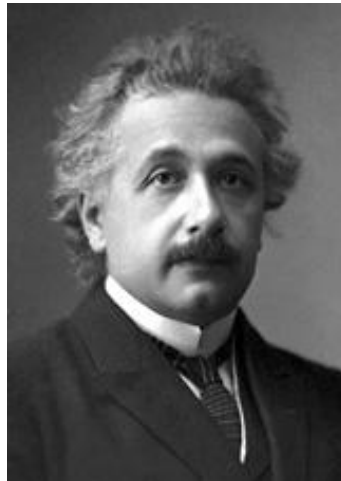
X-ray<sup>1</sup> Photoelectron spectroscopy, based on the photoelectric effect,<sup>2,3</sup> was developed in the mid-1960's as a practical technique by [Kai Siegbahn](#) and his research group at the University of Uppsala, Sweden.<sup>4</sup>



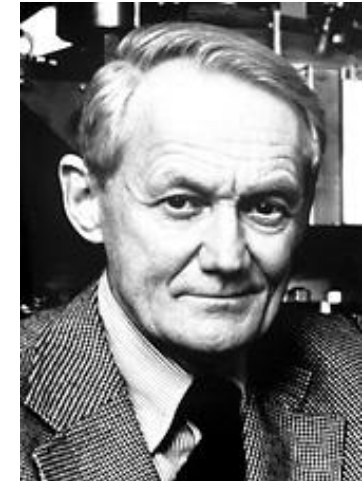
Wilhelm Conrad Röntgen



Heinrich Rudolf Hertz



Albert Einstein

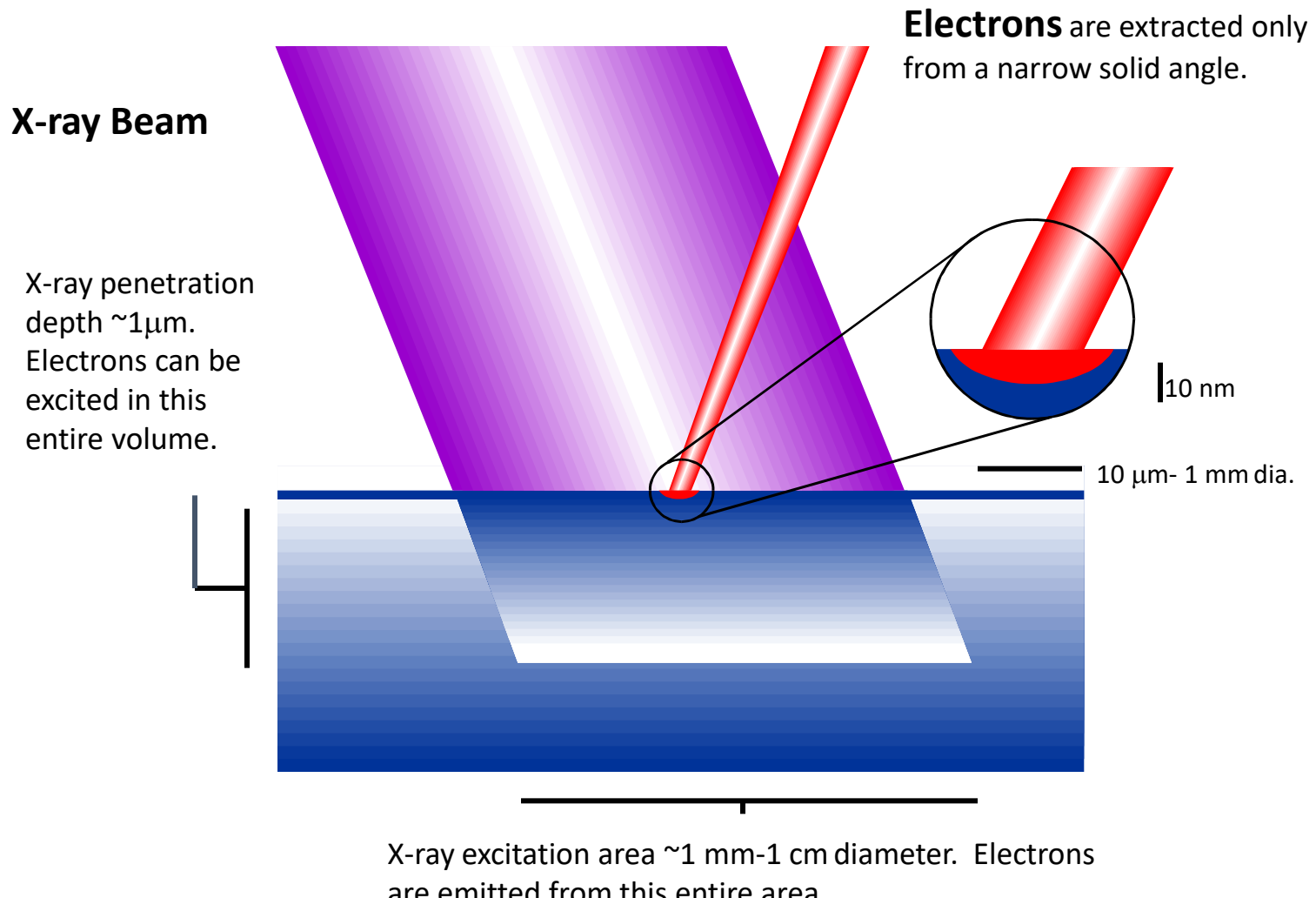


Kai M. Siegbahn



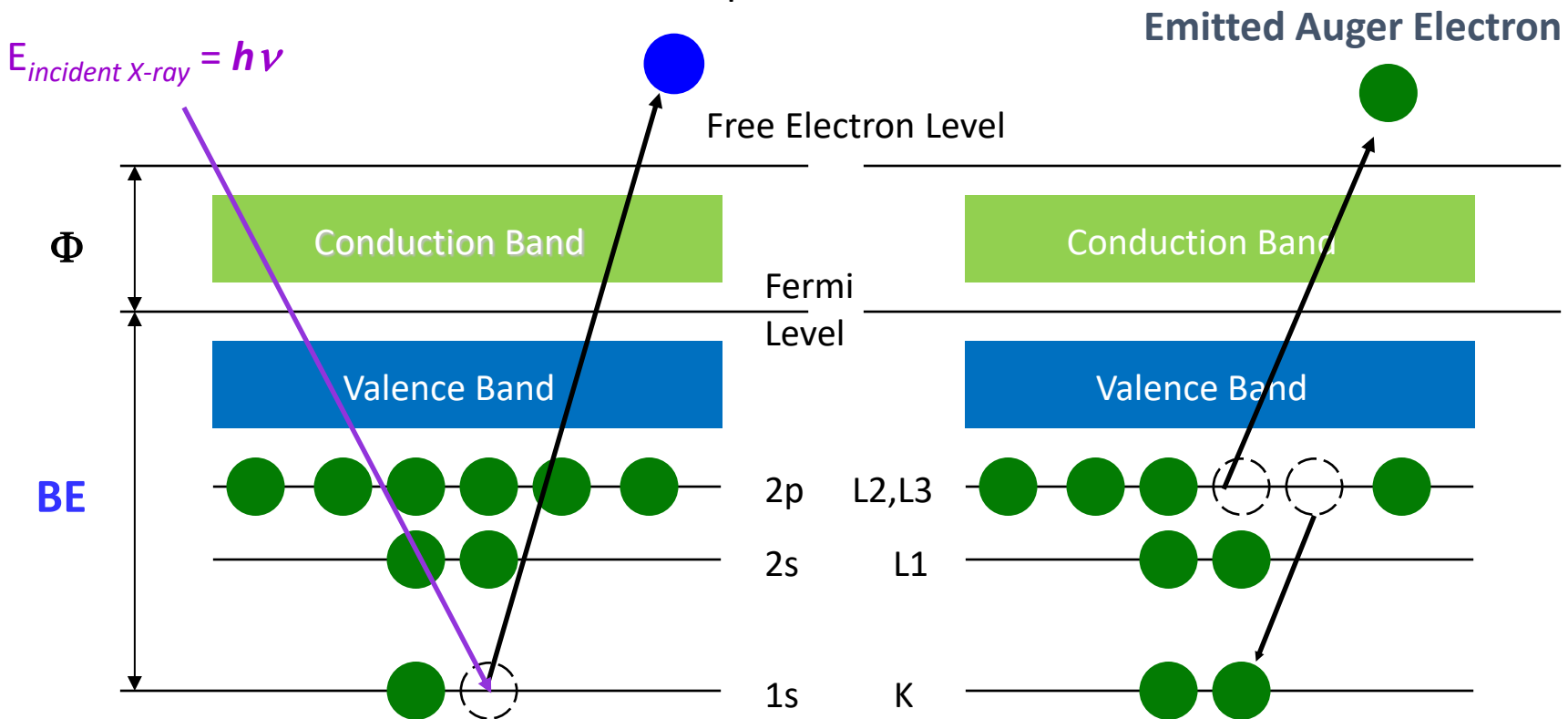
1. W. Röntgen, 1901 Nobel Prize in Physics "in recognition of the extraordinary services he has rendered by the discovery of the remarkable rays subsequently named after him."
2. H. Hertz, "Über einen Einfluss des ultravioletten Lichtes auf die electrische Entladung," *Ann. Physik* **31**, 983 (1887). The IEEE Heinrich Hertz Medal was established by the Board of Directors in 1987 "for outstanding achievements in Hertzian (radio) waves."
3. A. Einstein, "Über einen die Erzeugung und Verwandlung des Lichtes betreffenden heuristischen Gesichtspunkt," *Ann. Physik* **17**, 132 (1905). 1921 Nobel Prize in Physics "for his services to Theoretical Physics, and especially for his discovery of the law of the photoelectric effect."
4. K. Siegbahn, Et. Al., *Nova Acta Regiae Soc.Sci.*, Ser. IV, Vol. 20 (1967). 1981 Nobel Prize in Physics "for his contribution to the development of high resolution electron spectroscopy."

# X-ray Photoelectron Spectroscopy Small Area Detection



# Photoelectron and Auger Electron Emission

$$KE \text{ (measured)} = h\nu \text{ (known)} - BE - \Phi_{\text{spec}} \text{ (calibrated)}$$

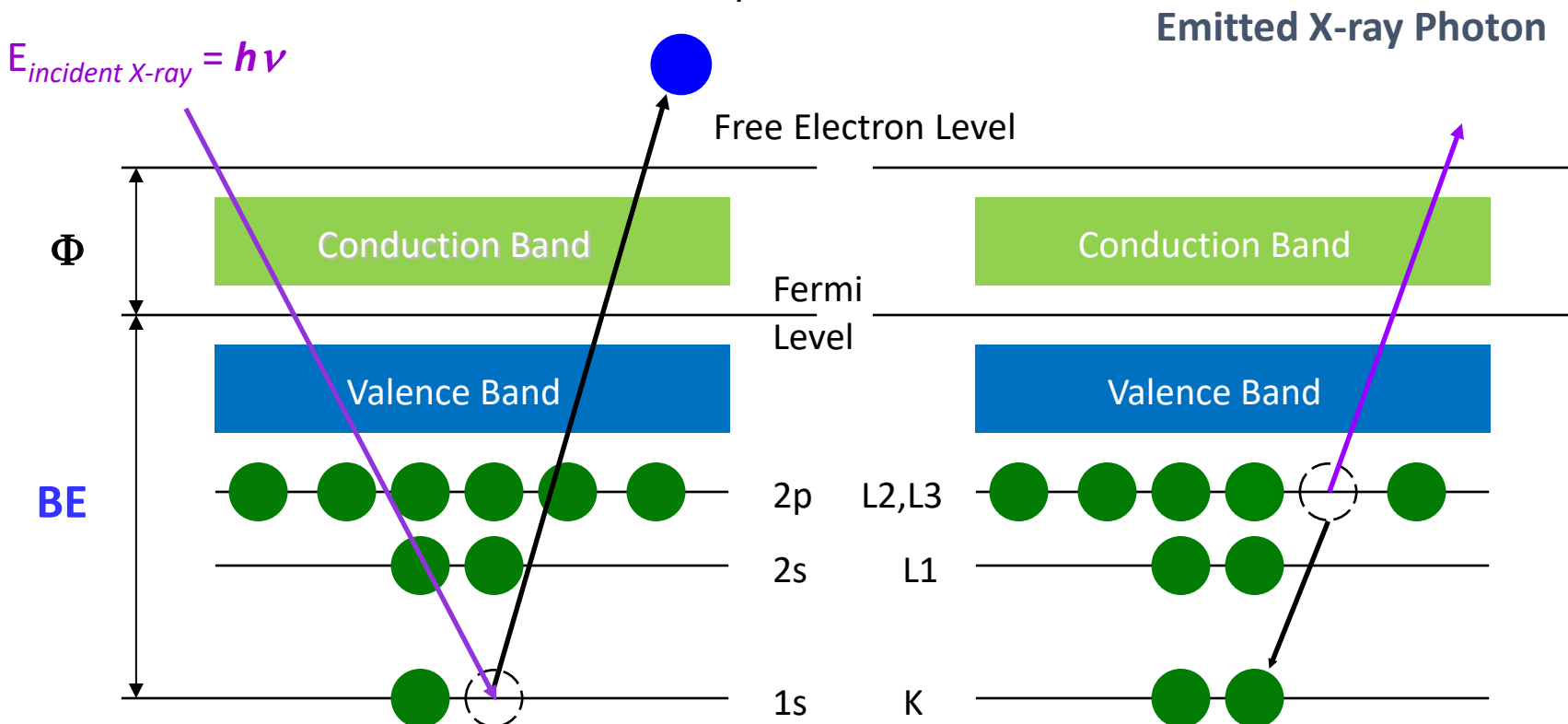


$$\text{Calculate: } BE = h\nu - KE - \Phi_{\text{spec}}$$

**BE – binding energy depends on Z, i.e. characteristic for the element**

# Photoelectron and Auger Electron Emission

$$KE \text{ (measured)} = h\nu \text{ (known)} - BE - \Phi_{\text{spec}} \text{ (calibrated)}$$



$$\text{Calculate: } BE = h\nu - KE - \Phi_{\text{spec}}$$

**BE – binding energy depends on Z, i.e. characteristic for the element**



# Photoelectron and Auger Electron Emission



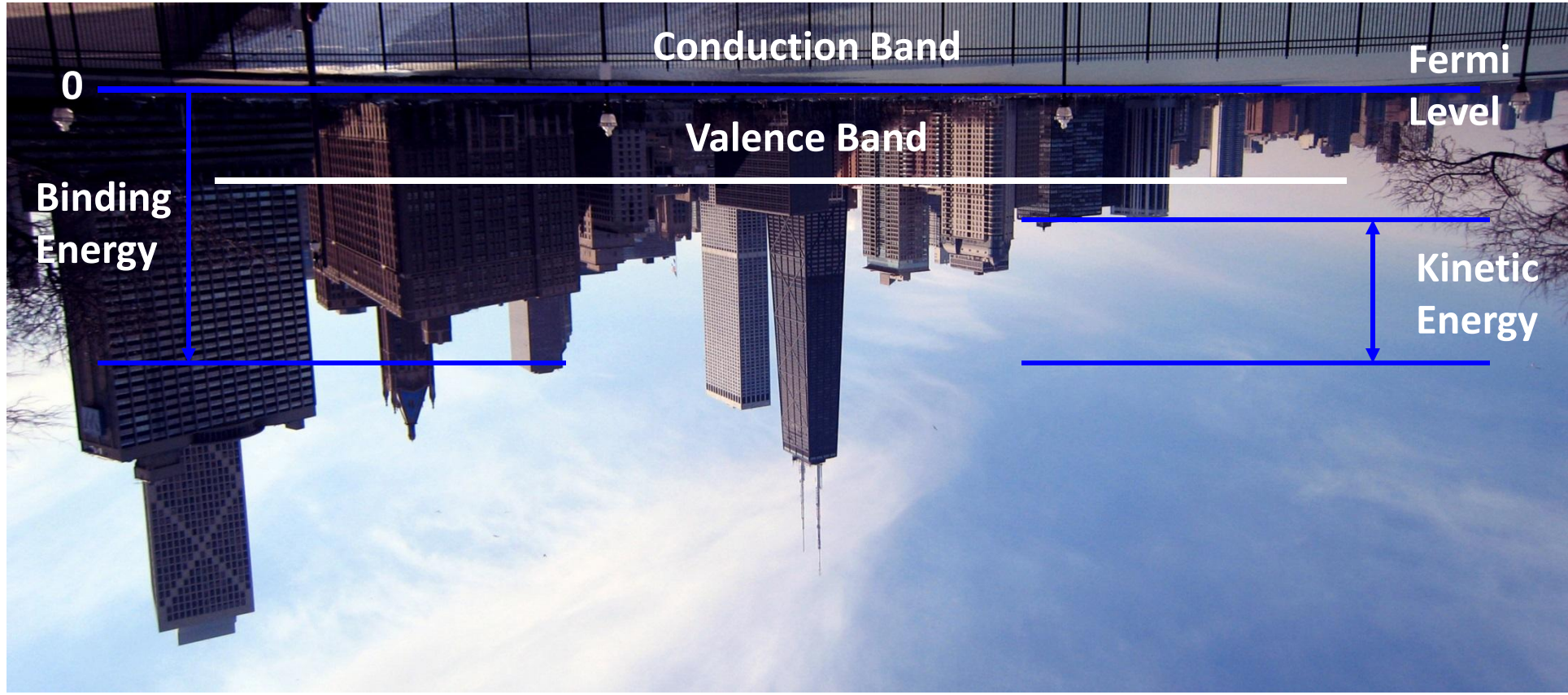
I

# Photoelectron and Auger Electron Emission



I

# Photoelectron and Auger Electron Emission



**Photoelectron Lines**

**Auger Electron Lines**

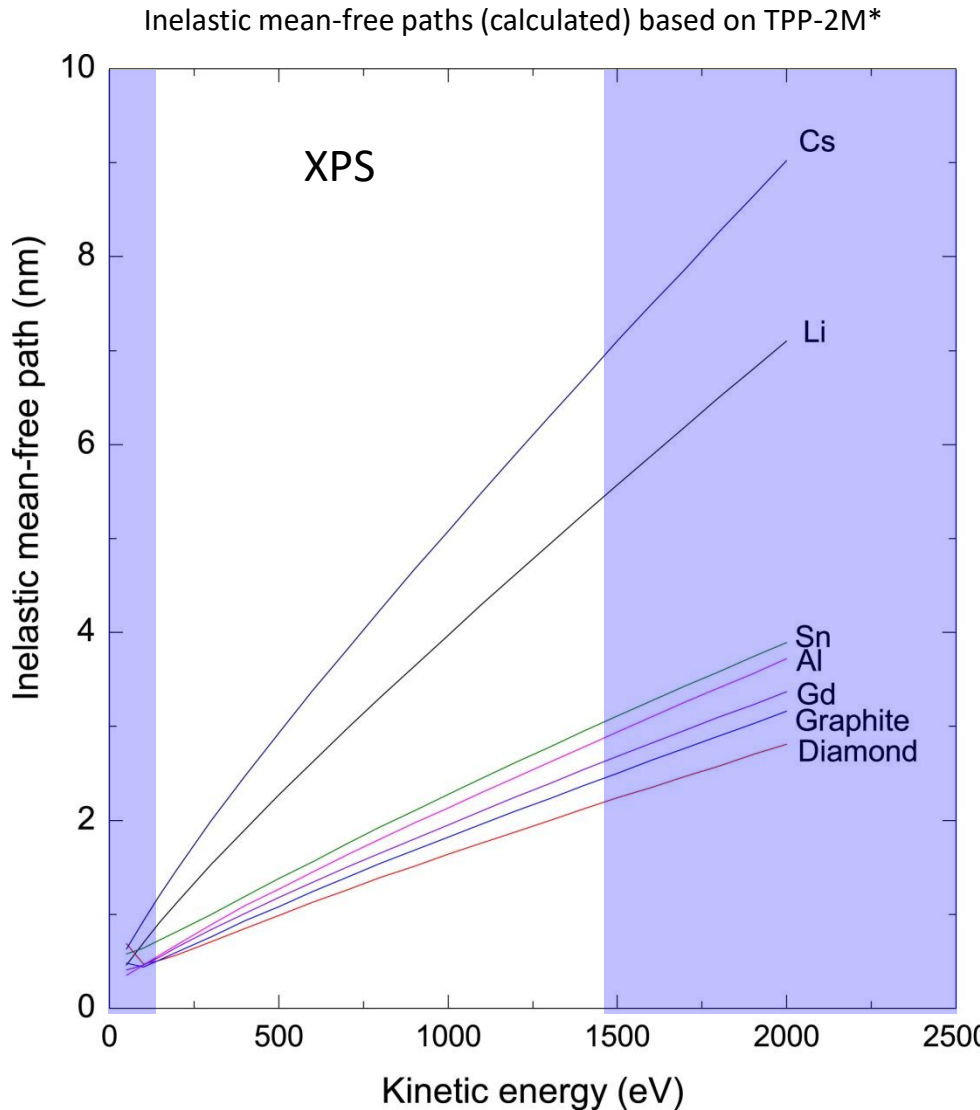
# Photoelectron and Auger Electron Emission



XPS can probe all of the orbitals in only the light elements.  
e.g. BE C 1s = 285 eV, Mg 1s = 1304 eV, Au 1s  $\approx$  81000 eV

# Surface Sensitivity: Electron Spectroscopy

**Inelastic Mean-Free Path:** The mean distance an electron can travel between inelastic scattering events.



Electrons travel only a few nanometers through solids.

\*S. Tanuma, C. J. Powell, D. R. Penn, *Surface and Interface Analysis*, **36**, 1 (2004).

# Surface Sensitivity: Electron Spectroscopy

## Assuming Inelastic Scattering Only

**Beer-Lambert relationship:**

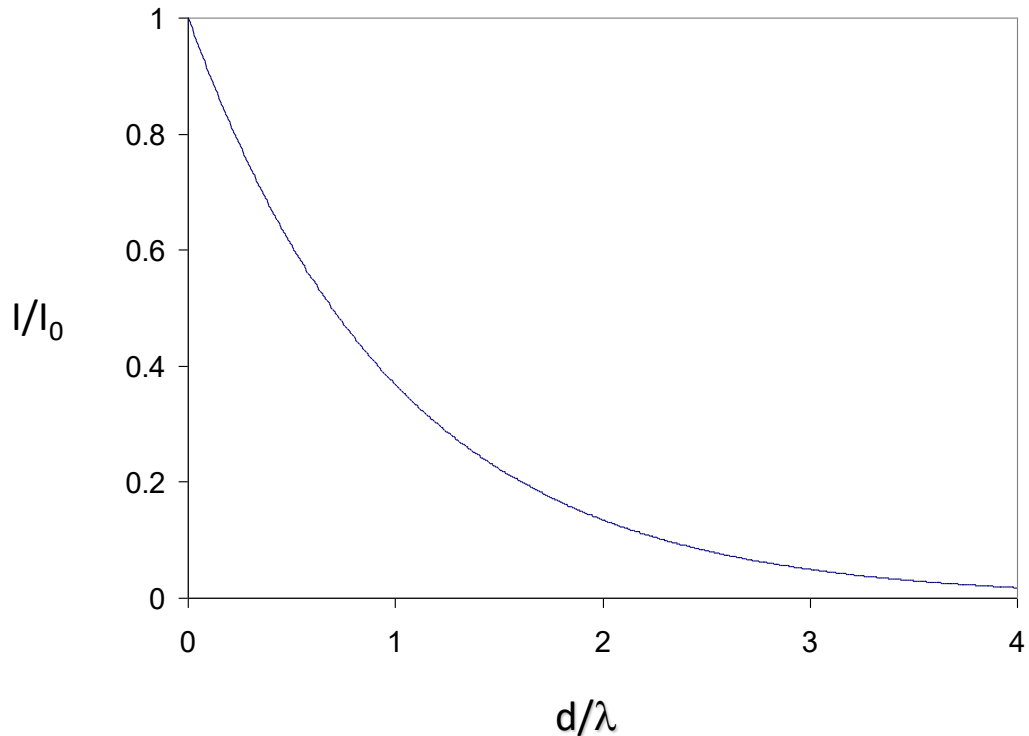
$$I = I_0 \exp(-d/\lambda \cos\theta)$$

where  $d$  = depth

$\lambda$  = Inelastic mean free path

at  $3\lambda$ ,  $I/I_0 = 0.05$

at 1000 eV,  $\lambda \approx 1.6 \text{ nm}$



**95% of the signal comes from within 5 nm of the surface or less!**



**Ratio: 100**

**Mt. Hood Prominence: 7707 feet**  
**Douglas Fir Height: ~77 feet**

**Ratio: 10000**

**Fingerprint Residue: ~50000 nm**  
**XPS Sensitivity: ~5 nm**

# Surface Sensitivity: Electron Spectroscopy

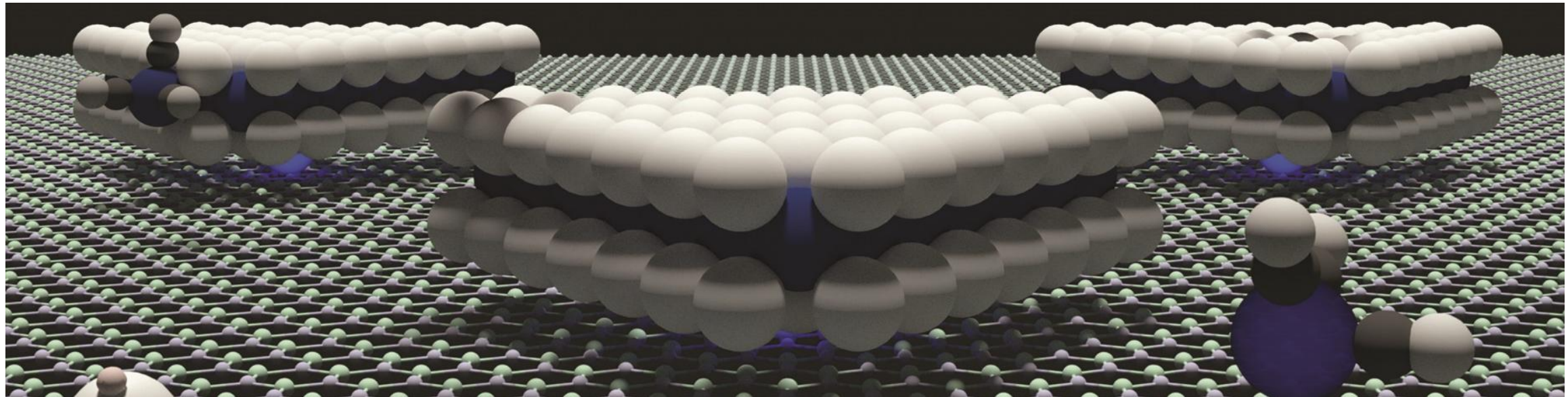
## X-ray Photoelectron Spectroscopy

### Advantage

Extremely surface sensitive!

### Disadvantage

Extremely surface sensitive!

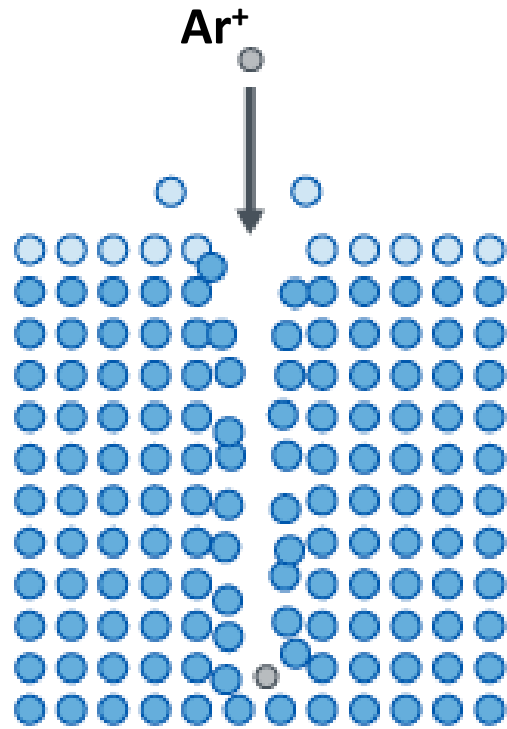


I

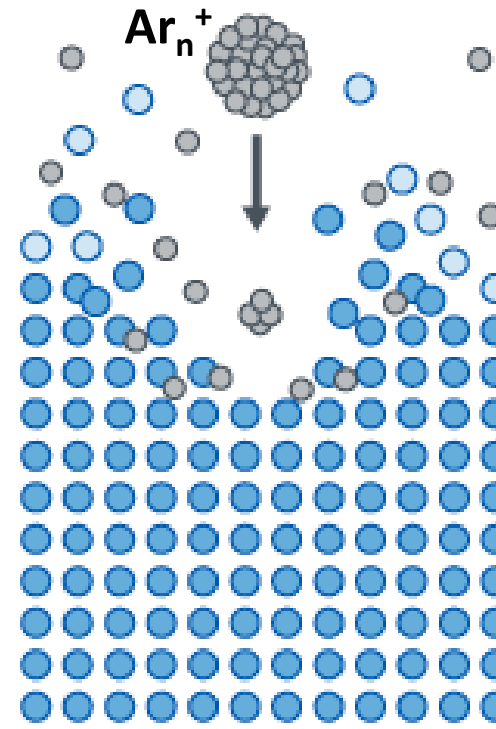
<https://phys.org/news/2019-05-substrate-defects-key-growth-d.html>

# Ion Sputtering

## Single atomic ion beam



## Cluster ion beam

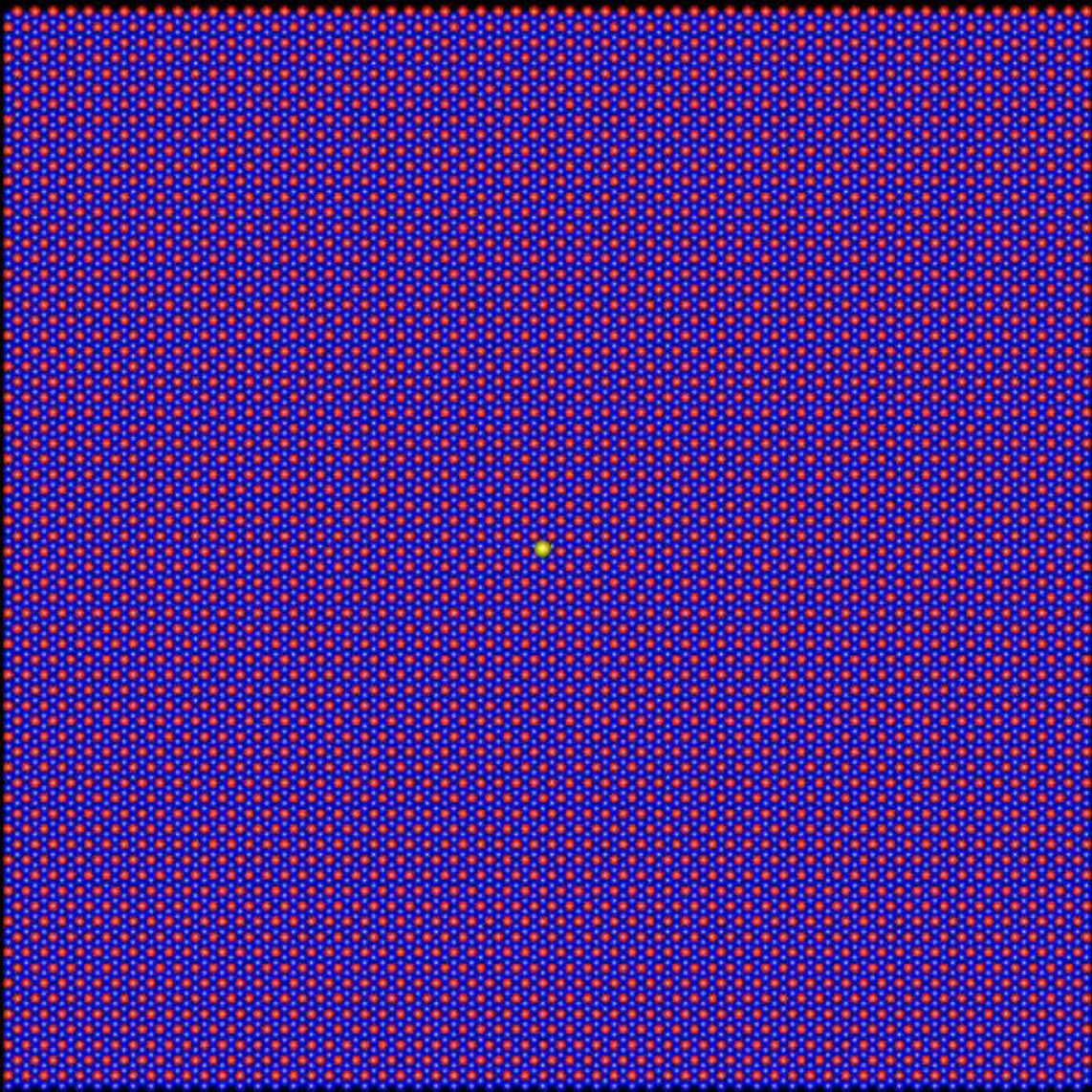


- Ions striking a surface interact with atoms in a series collisions.
- recoiled target atoms in turn collide with atom at rest generating a collision cascade.
- The initial ion energy and momentum are distributed among the target recoil atoms.
- When  $E_i > 1 \text{ keV}$ , the cascade is “linear,” i.e. approximated by a series of binary collisions in a stationary matrix.

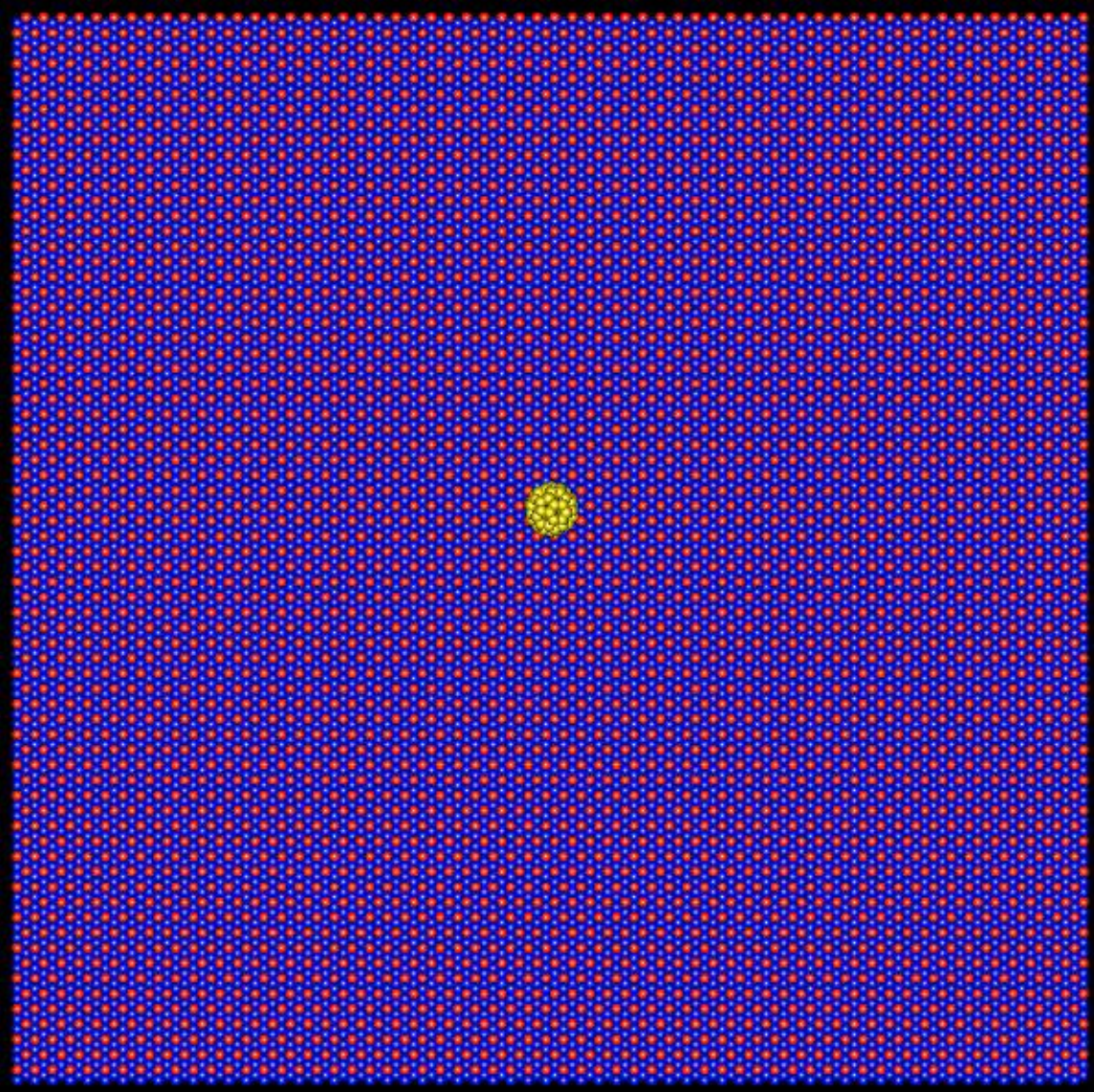
I

P. Sigmund, “Sputtering by ion bombardment: theoretical concepts,” in *Sputtering by particle bombardment I*, edited by R. Behrsh, Springer-Verlag, 1981.  
Image credit: <https://ulvac-phi.com/>

**15 KeV  $\text{Ga}^+$**



**15 KeV  $\text{C}_{60}^+$**



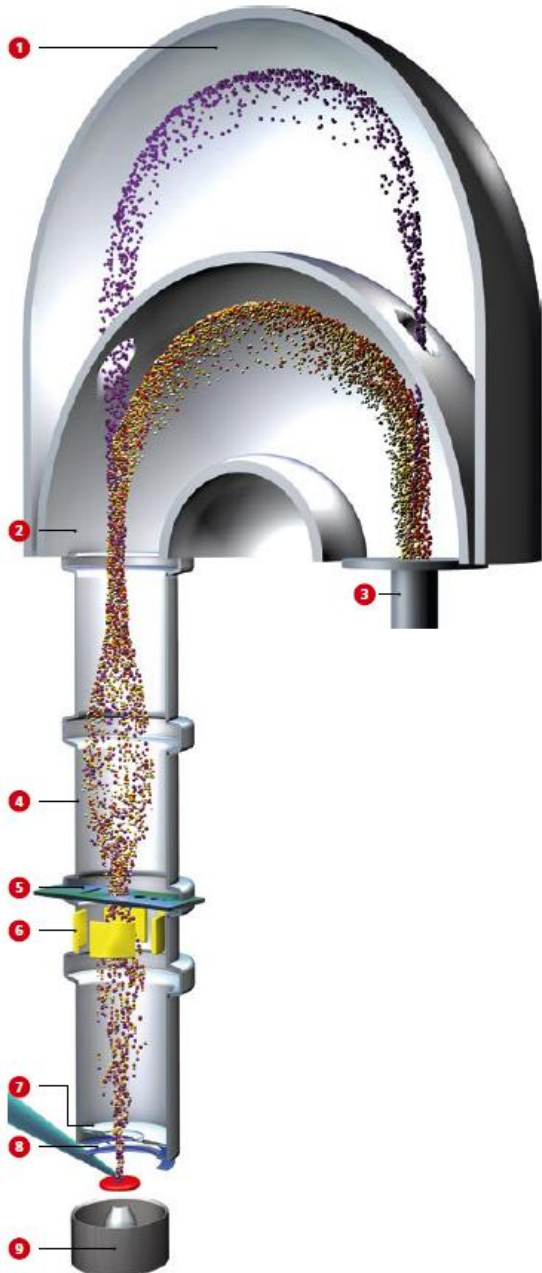


# X-ray Photoelectron Spectrometer

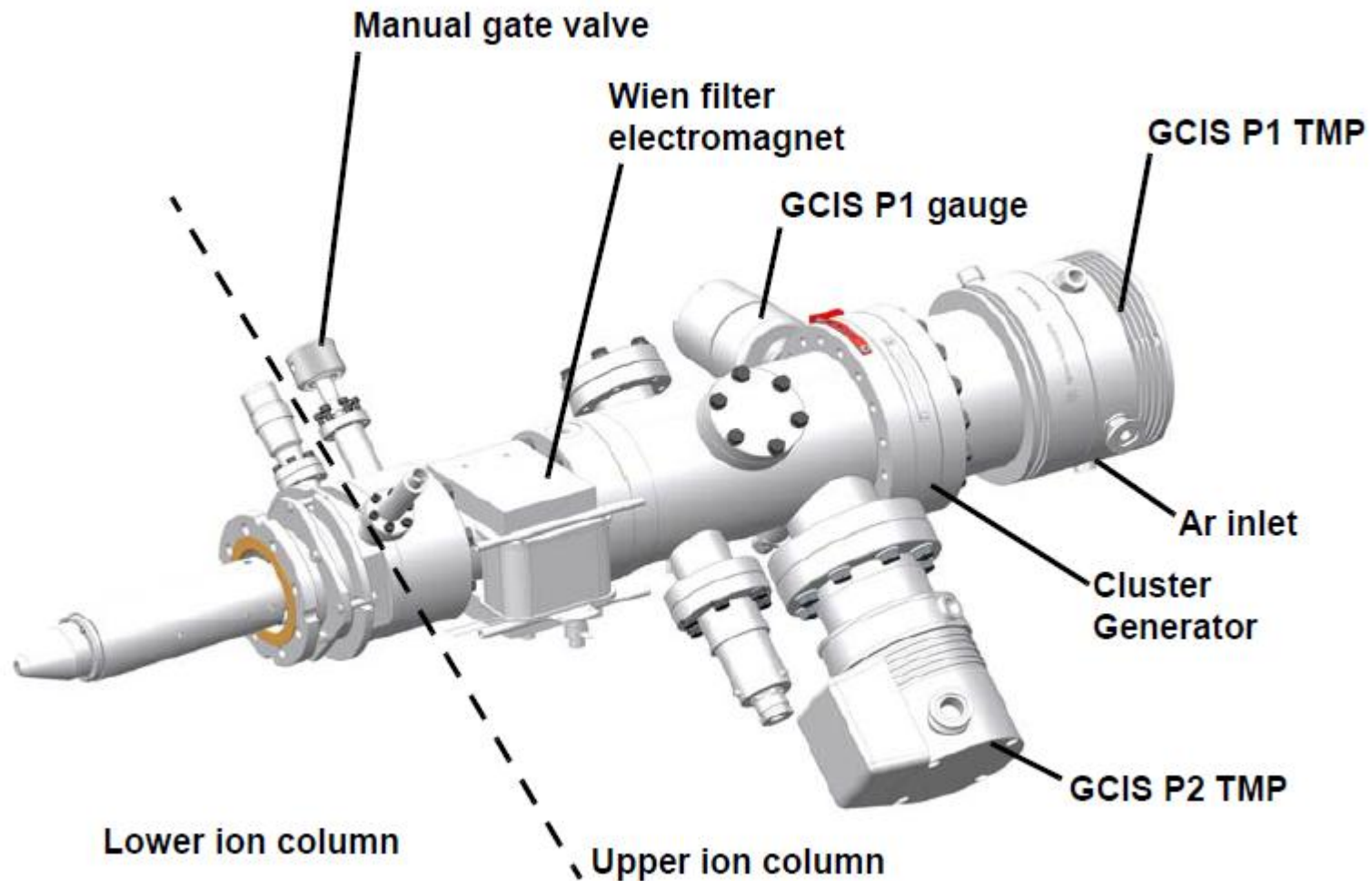


Image credit: <https://www.kratos.com/>

- ① Spherical mirror analyser
- ② Hemispherical analyser
- ③ Delay-line detector
- ④ Electrostatic lens
- ⑤ Selected area aperture drive
- ⑥ Octopole scan plates
- ⑦ Variable iris drive
- ⑧ Charge neutraliser
- ⑨ Magnetic lens

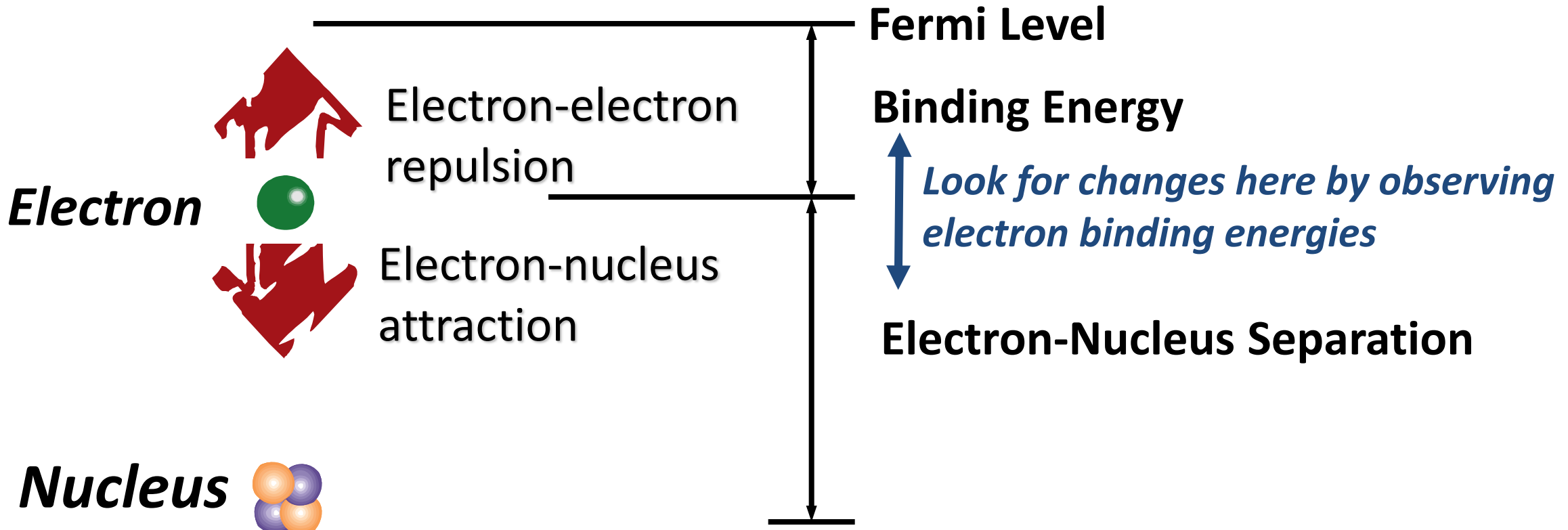


# Gas-cluster ion Source (GCIS)



I

## Pure Element



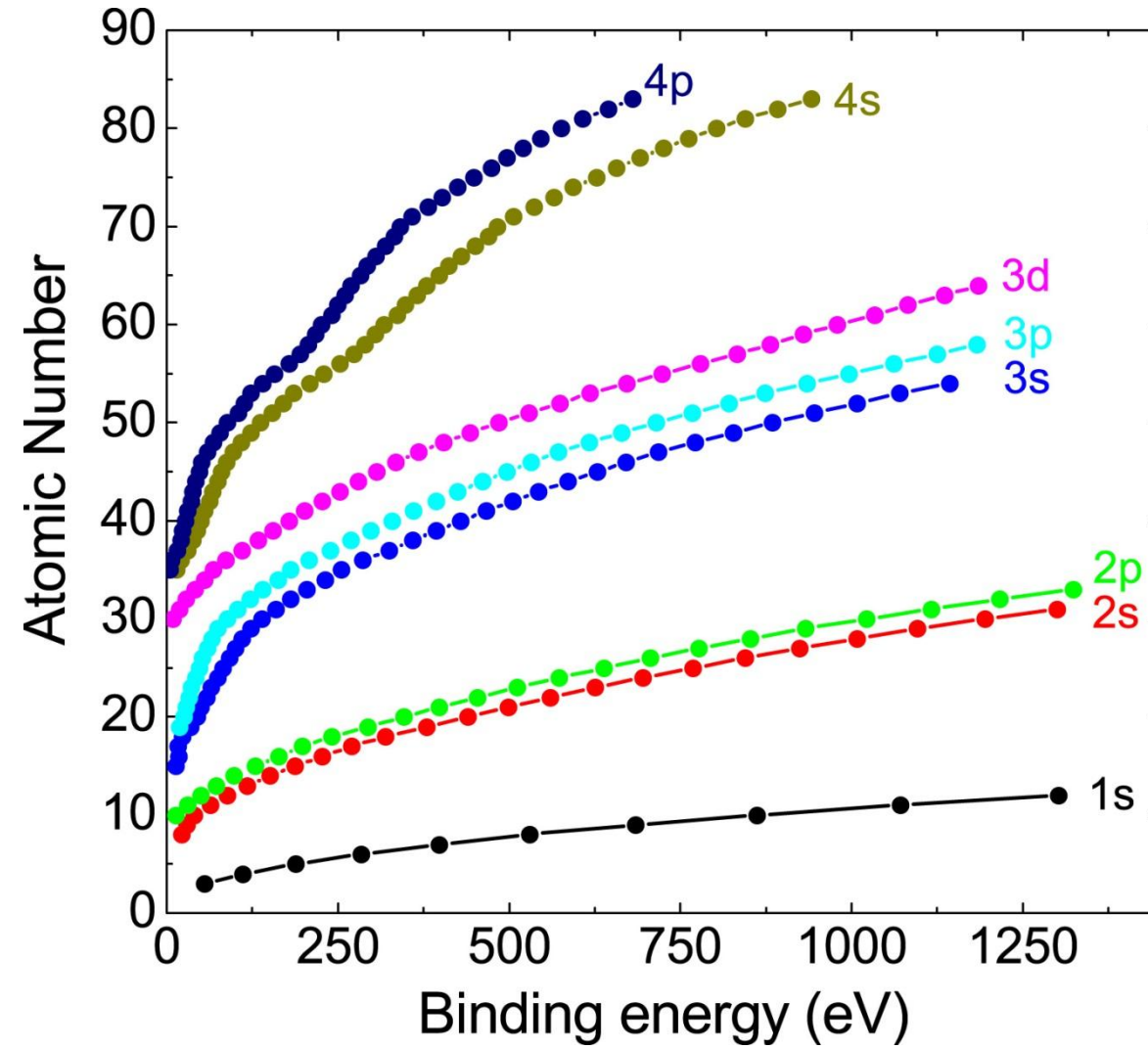
I

# Elemental Shifts

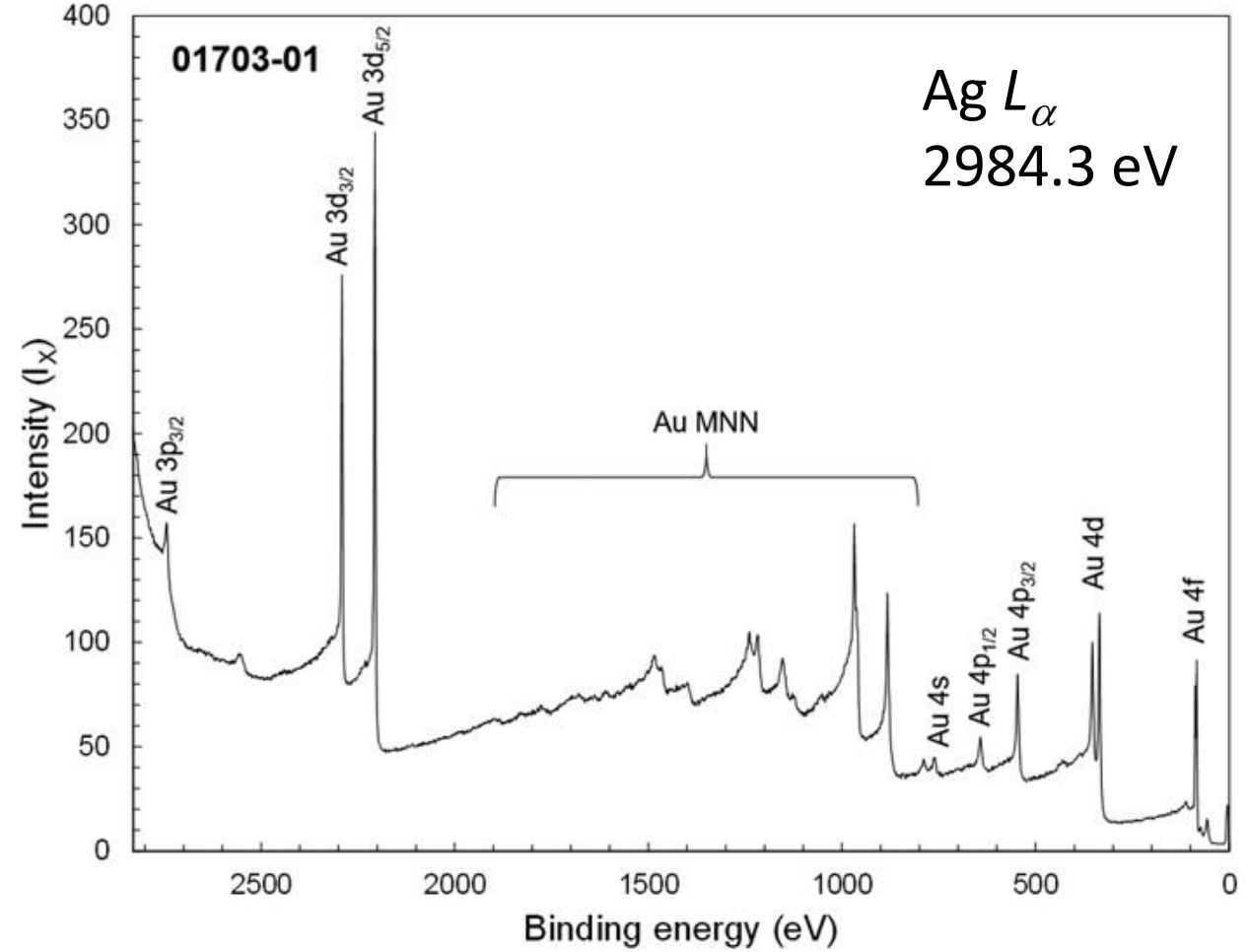
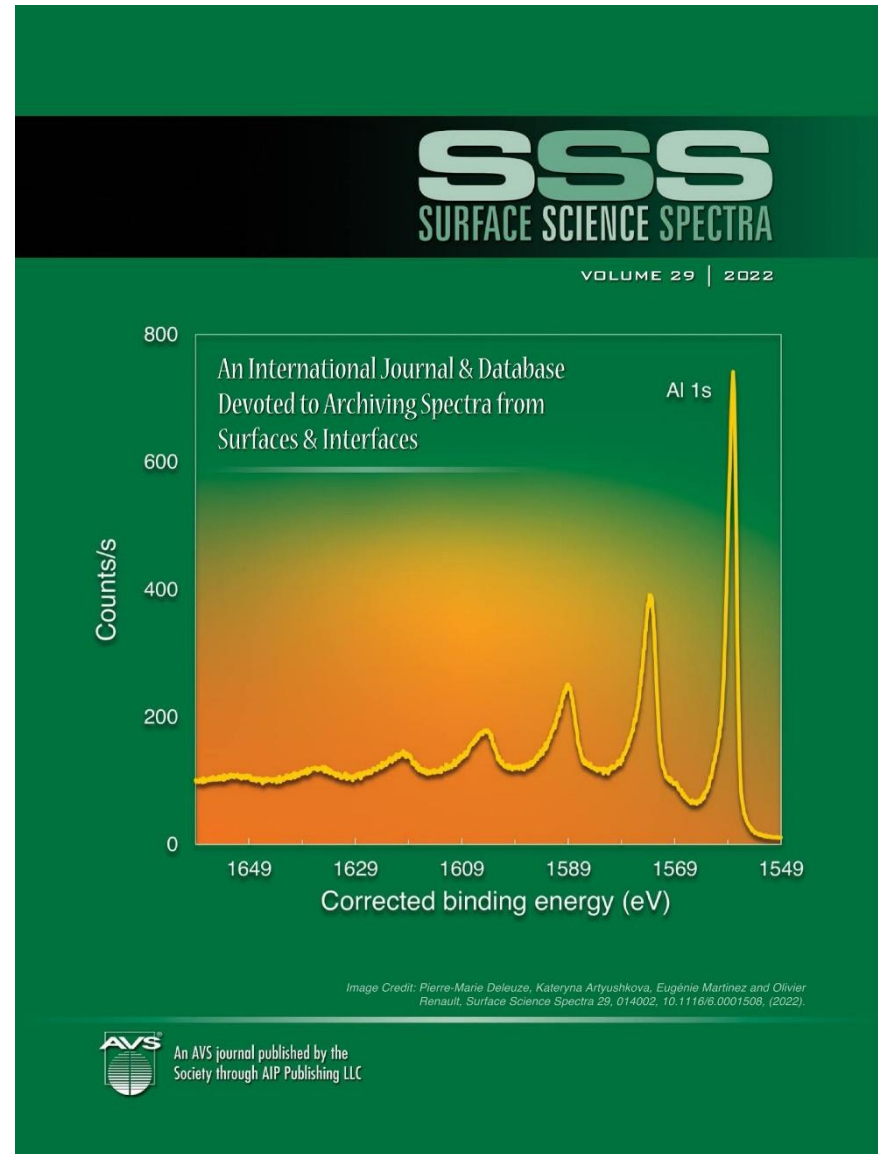
1 1IA 11A																				18 VIIIA 8A		
1 H Hydrogen 1.0079	2 Be Beryllium 9.01218	3 Li Lithium 6.941	4 Be Beryllium 9.01218	5 B Boron 10.811	6 C Carbon 12.011	7 N Nitrogen 14.00674	8 O Oxygen 15.9994	9 F Fluorine 18.998403	10 Ne Neon 20.1797	13 Al Aluminum 26.981539	14 Si Silicon 28.0855	15 P Phosphorus 30.973762	16 S Sulfur 32.066	17 Cl Chlorine 35.4527	18 Ar Argon 39.948							
3 Na Sodium 22.989768	11 Mg Magnesium 24.305	3 IIIIB 3B	4 IVB 4B	5 VB 5B	6 VIB 6B	7 VIIIB 7B	8 VIII 8	9 VIII 8	10	11 IB 1B	12 IIB 2B											
19 K Potassium 39.0983	20 Ca Calcium 40.078	21 Sc Scandium 44.95591	22 Ti Titanium 47.88	23 V Vanadium 50.9415	24 Cr Chromium 51.9961	25 Mn Manganese 54.938	26 Fe Iron 55.847	27 Co Cobalt 58.9332	28 Ni Nickel 58.6934	29 Cu Copper 63.546	30 Zn Zinc 65.39	31 Ga Gallium 69.732	32 Ge Germanium 72.64	33 As Arsenic 74.92159	34 Se Selenium 78.96	35 Br Bromine 79.904	36 Kr Krypton 83.80					
37 Rb Rubidium 85.4678	38 Sr Strontium 87.62	39 Y Yttrium 88.90585	40 Zr Zirconium 91.224	41 Nb Niobium 92.90638	42 Mo Molybdenum 95.94	43 Tc Technetium 98.9072	44 Ru Ruthenium 101.07	45 Rh Rhodium 102.9055	46 Pd Palladium 106.42	47 Ag Silver 107.8682	48 Cd Cadmium 112.411	49 In Indium 114.818	50 Sn Tin 118.71	51 Sb Antimony 121.760	52 Te Tellurium 127.6	53 I Iodine 126.90447	54 Xe Xenon 131.29					
55 Cs Cesium 132.90543	56 Ba Barium 137.327	57-71	72 Hf Hafnium 178.49	73 Ta Tantalum 180.9479	74 W Tungsten 183.85	75 Re Rhenium 186.207	76 Os Osmium 190.23	77 Ir Iridium 192.22	78 Pt Platinum 195.08	79 Au Gold 196.9665	80 Hg Mercury 200.59	81 Tl Thallium 204.3833	82 Pb Lead 207.2	83 Bi Bismuth 208.98037	84 Po Polonium [208.9824]	85 At Astatine 209.9871	86 Rn Radon 222.0176					
87 Fr Francium 223.0197	88 Ra Radium 226.0254	89-103	104 Rf Rutherfordium [261]	105 Db Dubnium [262]	106 Sg Seaborgium [266]	107 Bh Bohrium [264]	108 Hs Hassium [269]	109 Mt Meitnerium [268]	110 Ds Darmstadtium [269]	111 Rg Roentgenium [272]	112 Cn Copernicium [277]	113 Uut Ununtrium unknown	114 Uuo Ununquadium [280]	115 Uup Ununpentium unknown	116 Uuh Ununhexium [298]	117 Uus Ununseptium unknown	118 Uuo Ununoctium unknown					
Lanthanide Series																						
Actinide Series																						
Alkali Metal      Alkaline Earth      Transition Metal      Basic Metal      Semimetals      Nonmetals      Halogens      Noble Gas      Lanthanides      Actinides																						

# Elemental Shifts

## Core Level Binding Energies

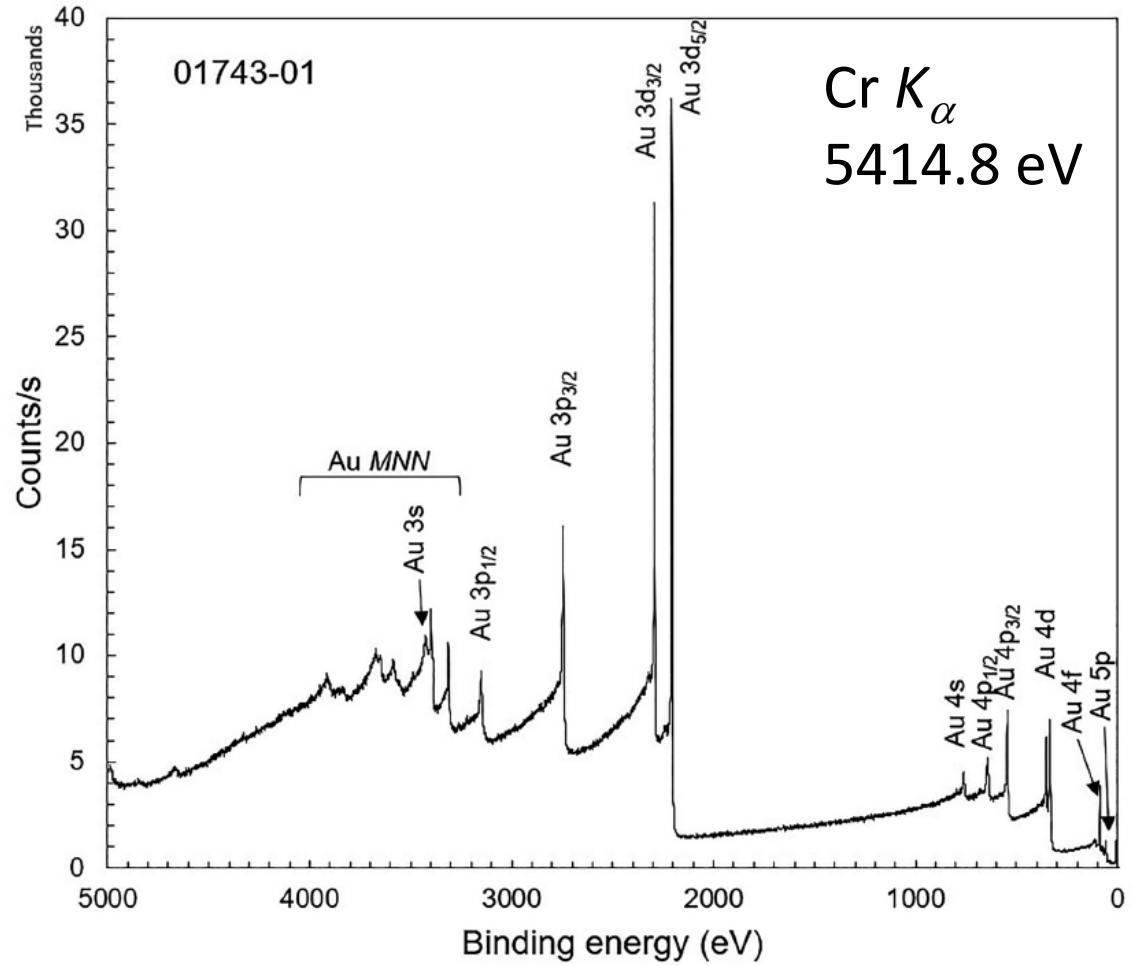
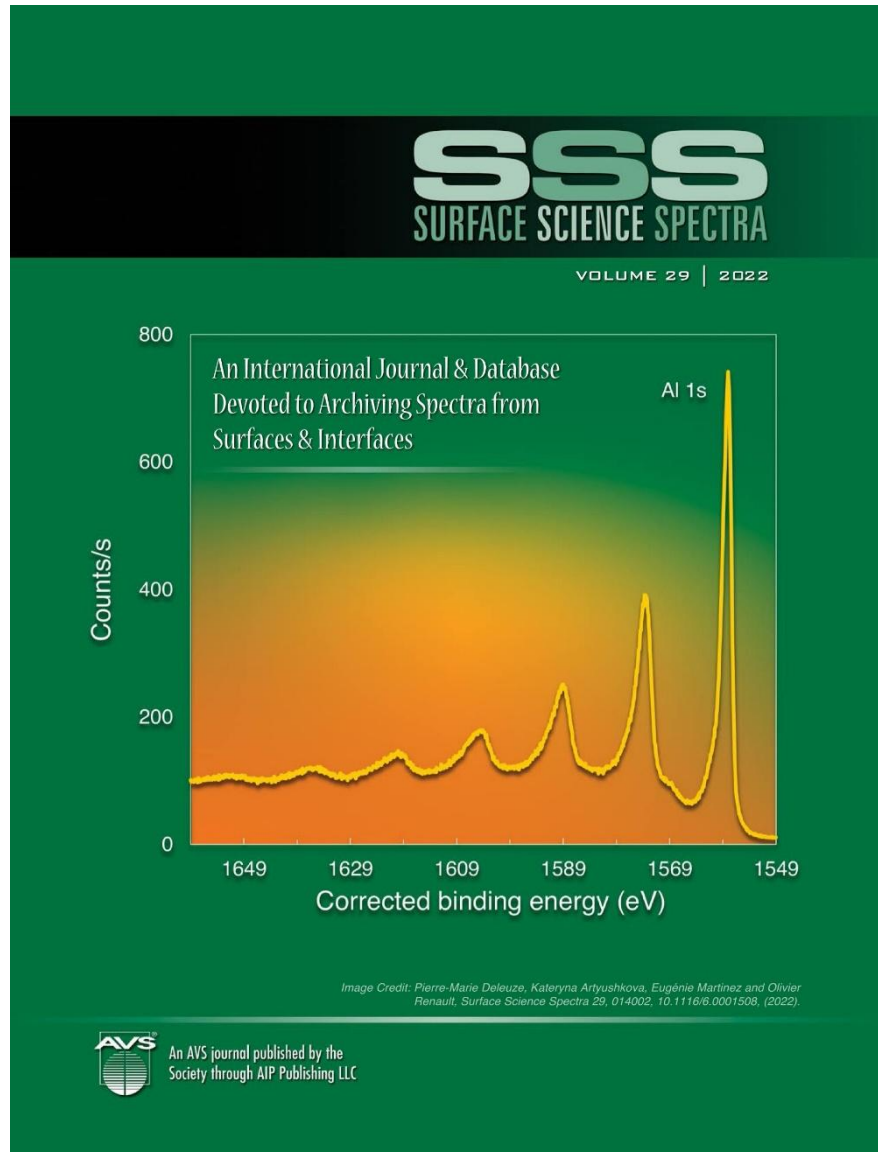


# Elemental Shifts – Higher Energy X-ray Sources



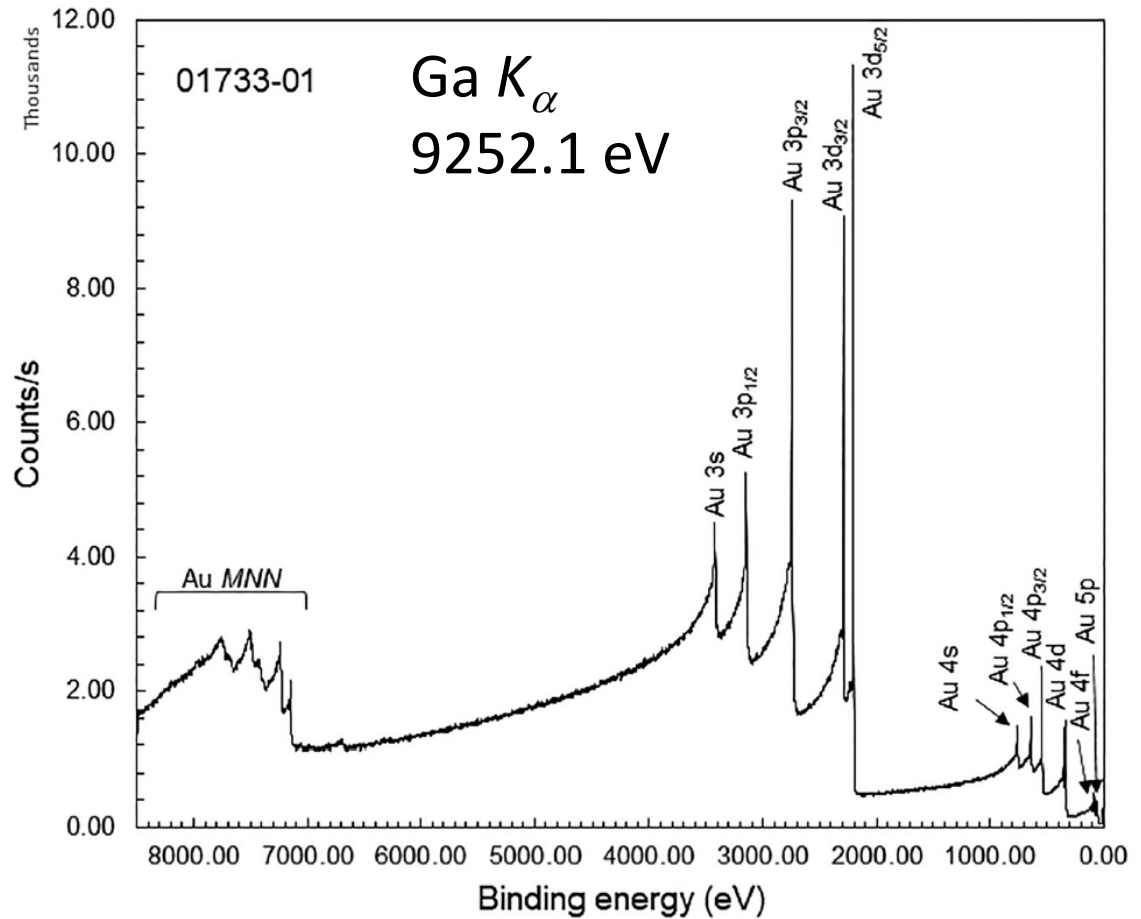
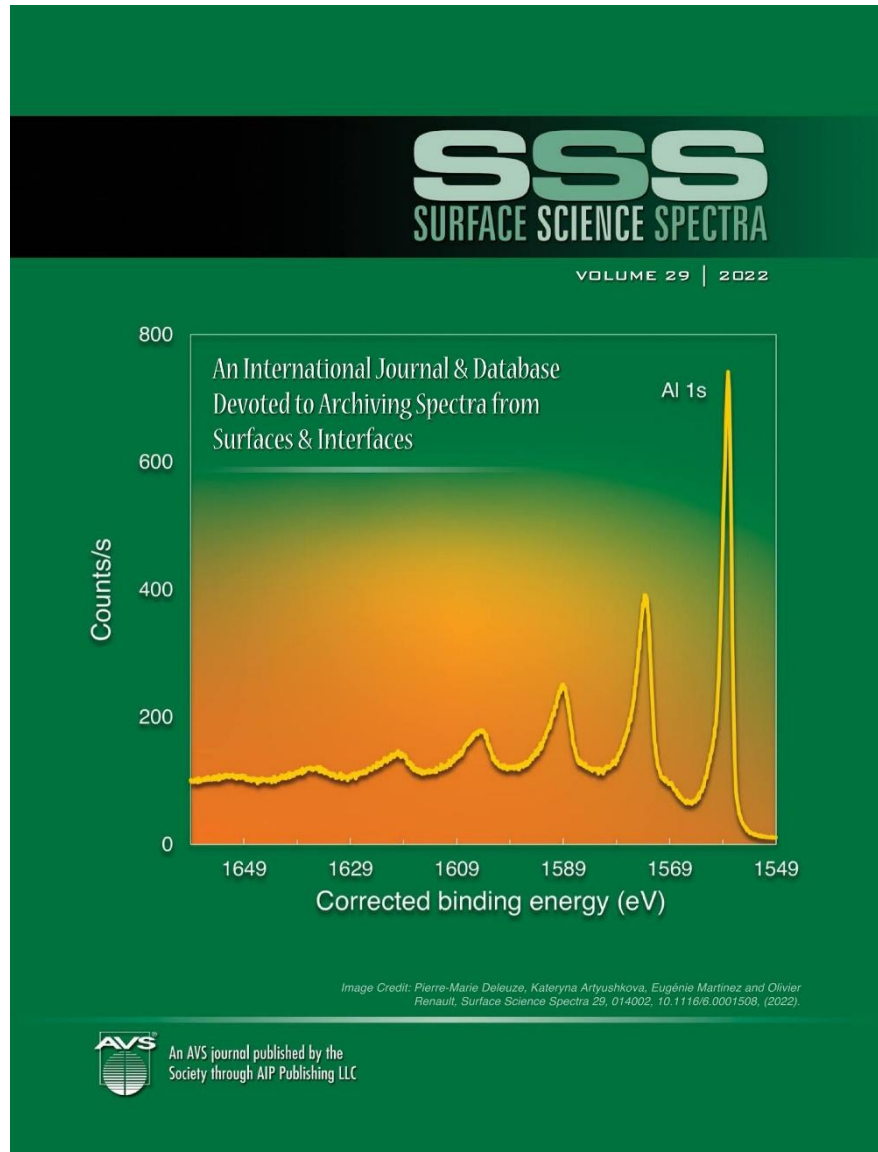
Jonathan D. P. Counsell; Alex G. Shard; David J. Cant; Christopher J. Blomfield; Parnia Navabpour; Xiaoling Zhang; *Surface Science Spectra* **28**, 024005 (2021). DOI: 10.1116/6.0001389  
Copyright © 2021 Author(s)

# Elemental Shifts – Higher Energy X-ray Sources



I. Hoflijk, A. Vanleenehove, I. Vaesen, C. Zborowski, K. Artyushkova, T. Conard; High energy x-ray photoelectron spectroscopy spectra of  $\text{Si}_3\text{N}_4$  measured by Cr  $K_{\alpha}$ . *Surface Science Spectra* 1 June 2022; 29 (1): 014013. <https://doi.org/10.1116/6.0001524>

# Elemental Shifts – Higher Energy X-ray Sources



Anja Vanleenhove, Fiona Crystal Mascarenhas, Ilse Hoflijk, Inge Vaesen, Charlotte Zborowski, Thierry Conard; HAXPES on SiO<sub>2</sub> with Ga K $\alpha$  photons. *Surface Science Spectra* 1 June 2022; 29 (1): 014012. <https://doi.org/10.1116/6.0001523>

# Elemental Shifts

## First-Row Transition Metals

3 IIIB 3B	4 IVB 4B	5 VB 5B	6 VIB 6B	7 VIIIB 7B	8	9 VIII 8	10	11 IB 1B	12 IIB 2B
21 <b>Sc</b> Scandium 44.95591	22 <b>Ti</b> Titanium 47.88	23 <b>V</b> Vanadium 50.9415	24 <b>Cr</b> Chromium 51.9961	25 <b>Mn</b> Manganese 54.938	26 <b>Fe</b> Iron 55.847	27 <b>Co</b> Cobalt 58.9332	28 <b>Ni</b> Nickel 58.6934	29 <b>Cu</b> Copper 63.546	30 <b>Zn</b> Zinc 65.39

### Binding Energy (eV)

Element	2p <sub>3/2</sub>	3p	Δ
Sc	399	29	370
Ti	454	33	421
V	512	37	475
Cr	574	43	531
Mn	639	48	591
Fe	707	53	654
Co	778	60	718
Ni	853	67	786
Cu	933	75	858
Zn	1022	89	933

I

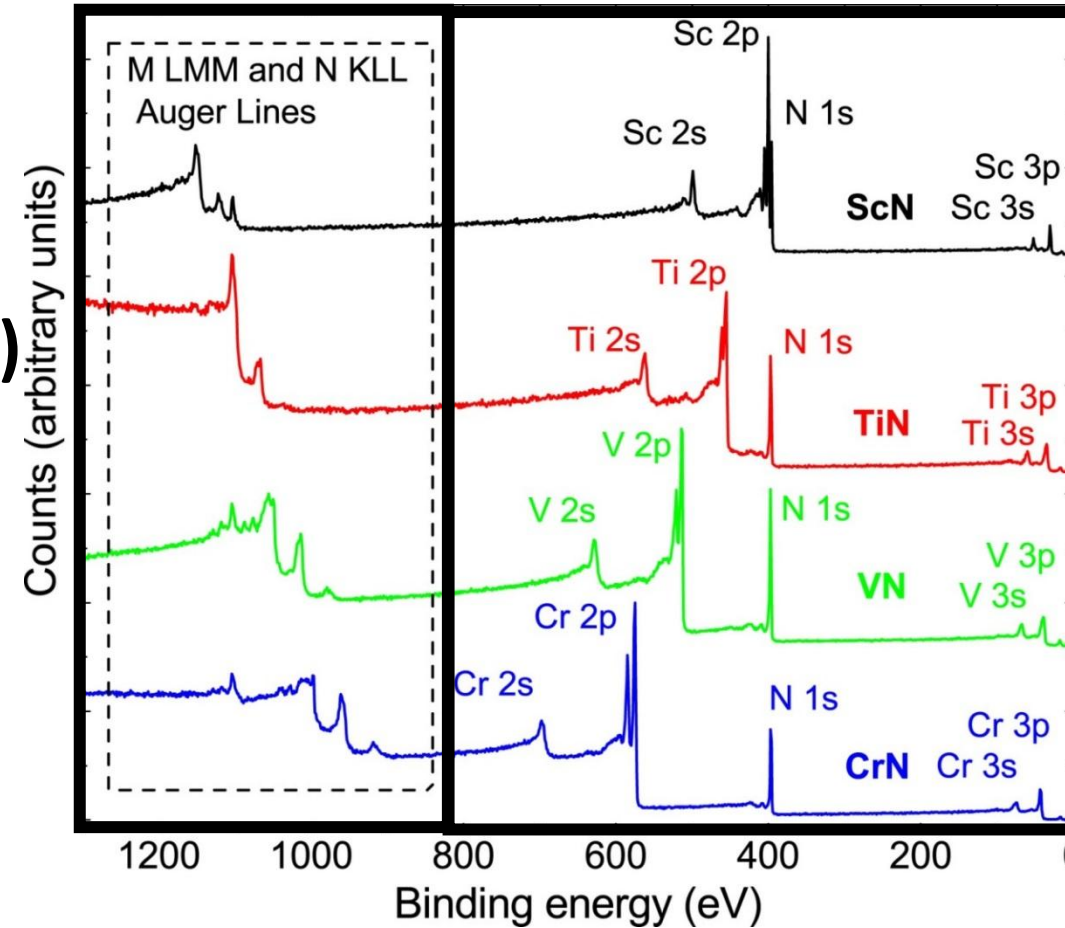
# Elemental Shifts: Transition Metal Nitrides

<sup>21</sup> Sc Scandium 44.95591	<sup>22</sup> Ti Titanium 47.88	<sup>23</sup> V Vanadium 50.9415	<sup>24</sup> Cr Chromium 51.9961
--	---------------------------------------	--	---

## First-Row Transition Metal Nitrides: ScN, TiN, VN, and CrN

Auger transition kinetic energies increase (binding energies decrease)

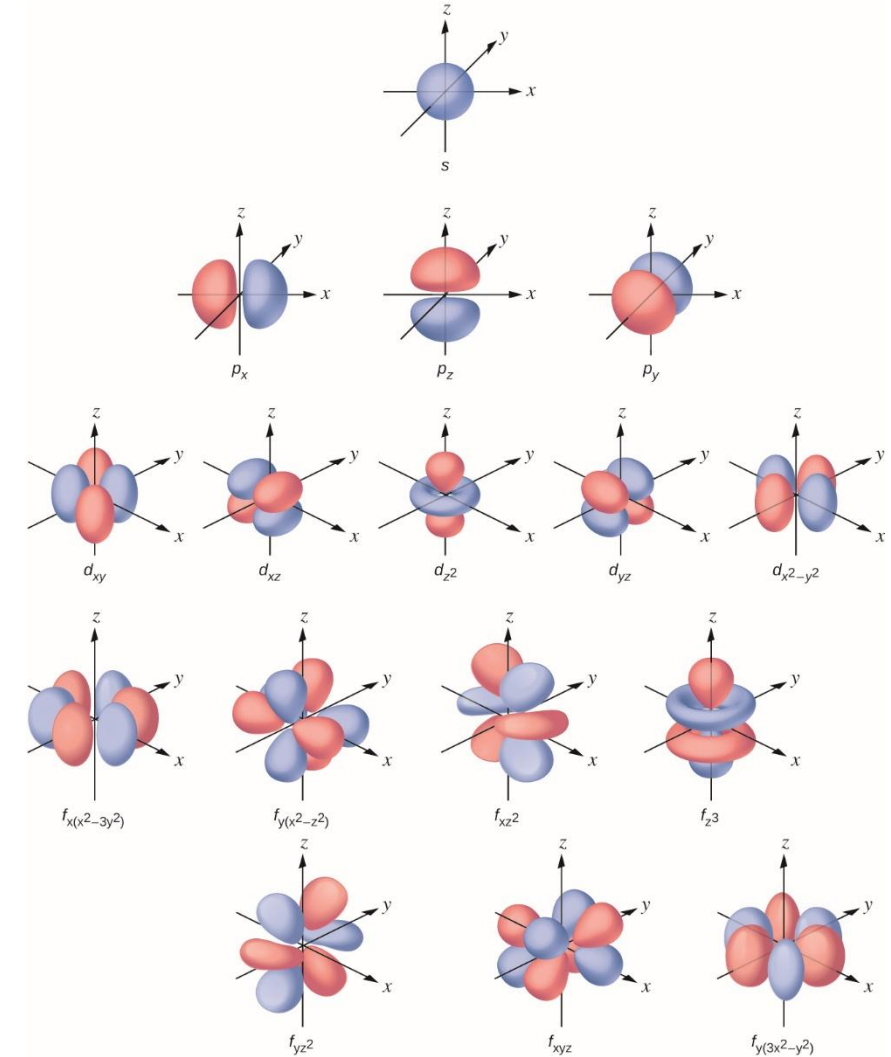
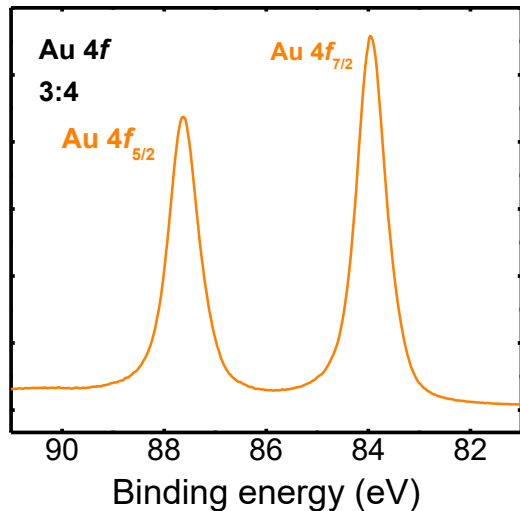
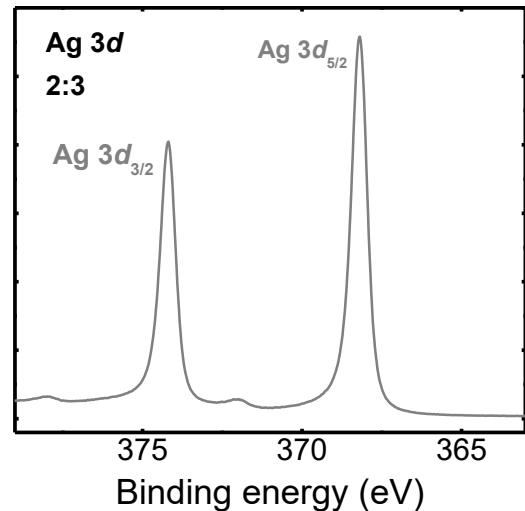
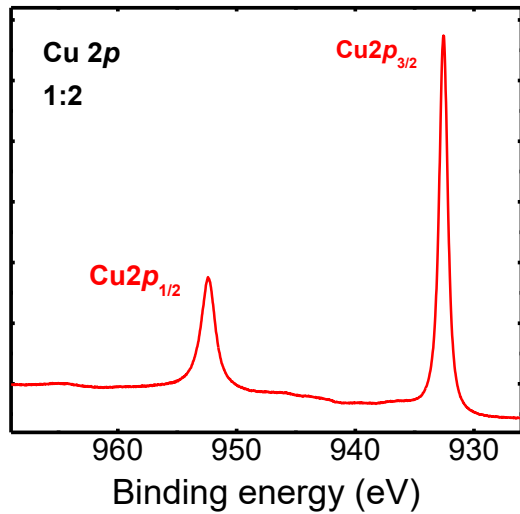
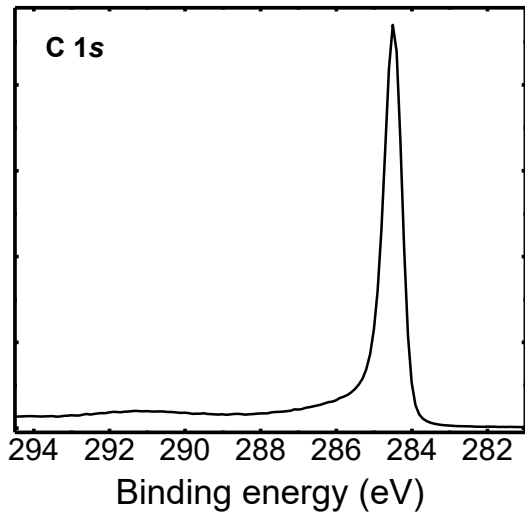
XPS Core-level binding energies increase



I

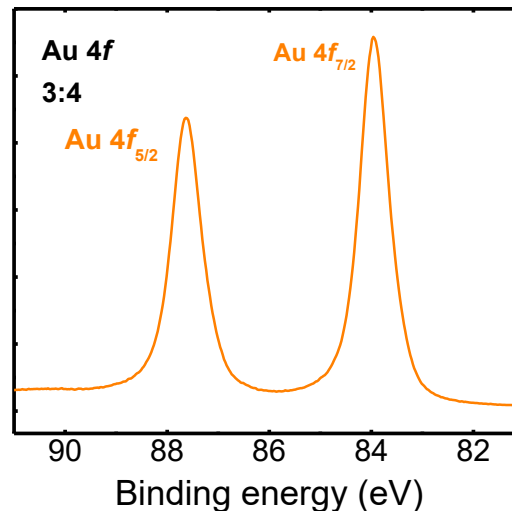
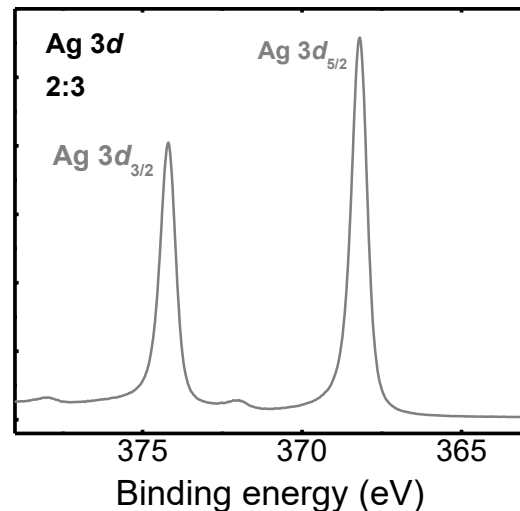
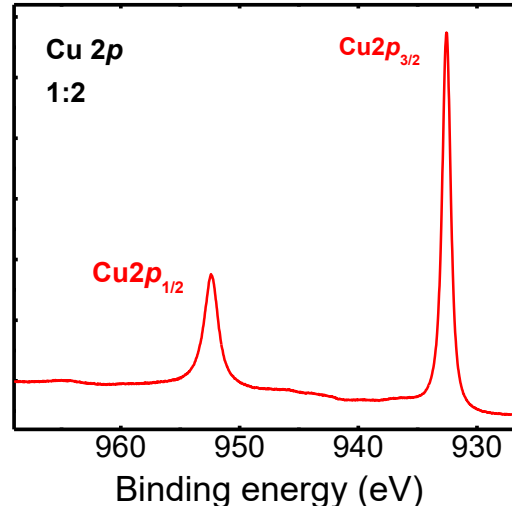
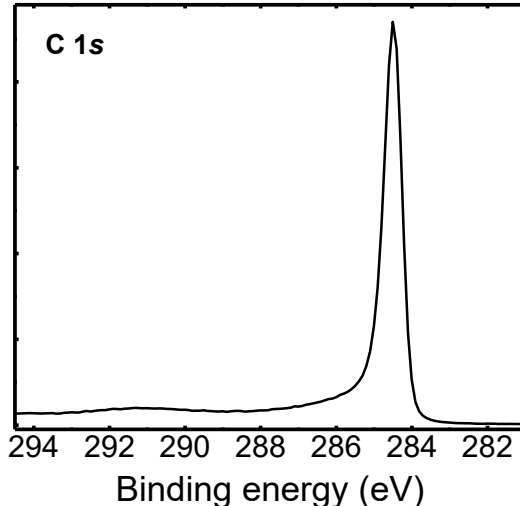
R. T. Haasch, T.-Y. Lee, D. Gall, C.-S. Shin, J. E. Greene, I. Petrov, *Surf. Sci. Spectra*, **7**, 169 (2000), *Surf. Sci. Spectra*, **7**, 193 (2000), *Surf. Sci. Spectra*, **7**, 221 (2000), *Surf. Sci. Spectra*, **7**, 250 (2000).

# Spin-orbit Splitting



R. T. Haasch, "X-ray Photoelectron Spectroscopy (XPS) and Auger Electron Spectroscopy (AES)," in *Practical Materials Characterization*, M. Sardela, ed., (Springer Science + Business Media, New York, 2014). ISBN 978-1-4614-9280-1. doi: 10.1007/978-1-4614-9281-8\_3.  
Atomic Orbitals and Quantum Numbers. (2019, June 5). <https://chem.libretexts.org/@go/page/122444>

# Spin-orbit Splitting



**Electron spin:  $s = \pm \frac{1}{2}$**

**Orbital angular momentum:  
 $l = 0, 1, 2, 3 \dots$  for  $s, p, d, f$  orbitals**

$$j = |l \pm s|$$

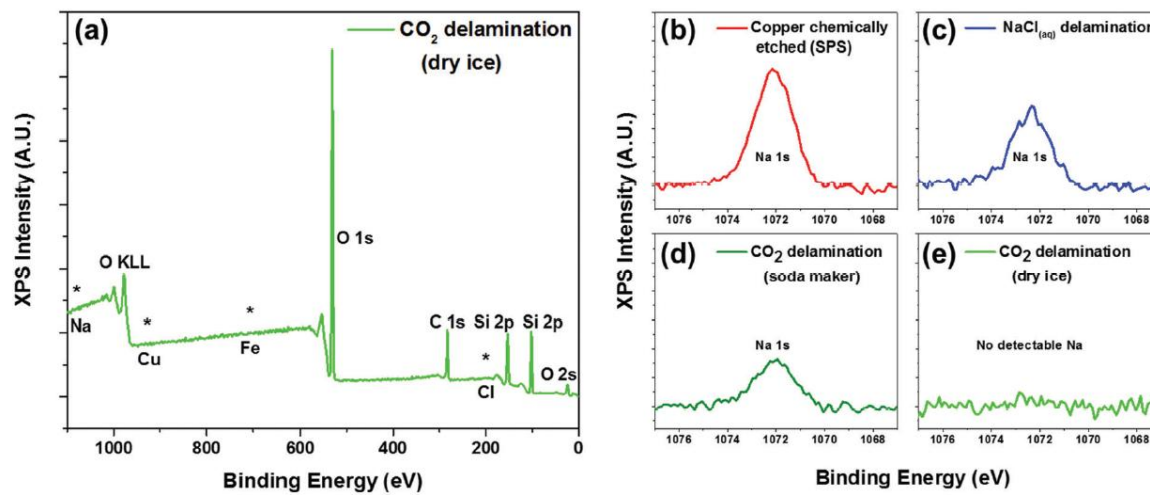
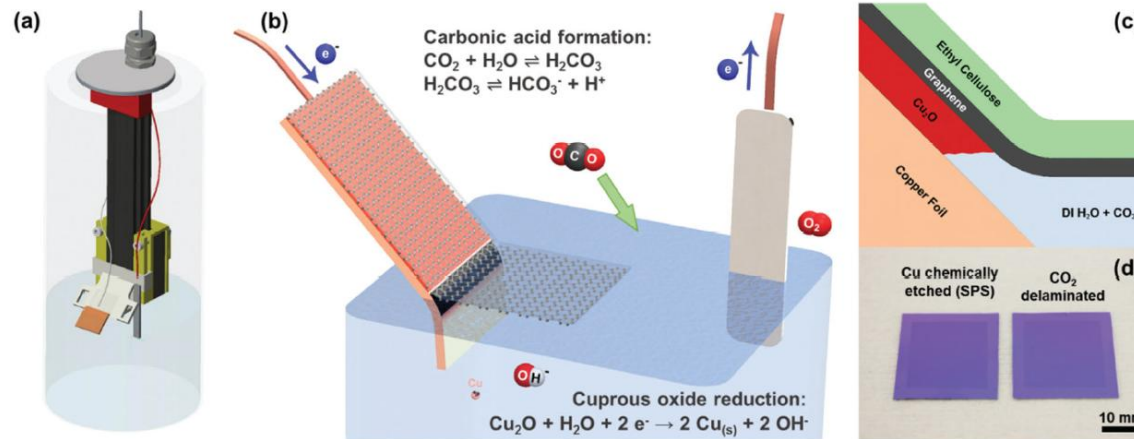
**Momentum quantum number:  
 $m_j, -j$  to  $j$  ( $2j + 1$  states)**



R. T. Haasch, "X-ray Photoelectron Spectroscopy (XPS) and Auger Electron Spectroscopy (AES)," in *Practical Materials Characterization*, M. Sardela, ed., (Springer Science + Business Media, New York, 2014). ISBN 978-1-4614-9280-1. doi: 10.1007/978-1-4614-9281-8\_3.  
Atomic Orbitals and Quantum Numbers. (2019, June 5). <https://chem.libretexts.org/@go/page/122444>

# Graphene Transfer

## A sustainable approach to large area transfer of graphene



- a) XPS survey of CO<sub>2</sub> delamination (from dry ice)
- b) Chemically etched (sodium persulphate)
- c) NaCl electrolyte delaminated
- d) CO<sub>2</sub> delamination using compressed CO<sub>2</sub> from soda maker
- e) Delamination using carbonic acid generated from dry ice pellets

M. C. Wang, W. Moestopo, S. Takekuma, S. Farabi, R. T. Haasch, S.-W. Nam, "Sustainable approach for large area transfer of graphene and recycle of the catalyst substrate," *J. Mater. Chem. C*, **5**, 11226 (2017). [doi:10.1039/c7tc02487h](https://doi.org/10.1039/c7tc02487h).

## Electronegativity Effects

### Carbon-Oxygen Bond

#### Oxygen Atom



**Valence Level**

C 2p



Electron-oxygen atom attraction  
(Oxygen Electronegativity)

**Core Level**

C 1s

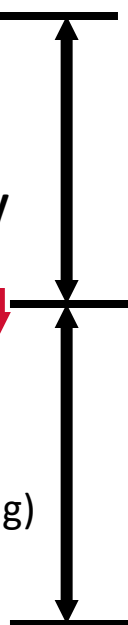


**C 1s Binding Energy**

Shift to higher binding energy



**Carbon Nucleus**



Electronegativity

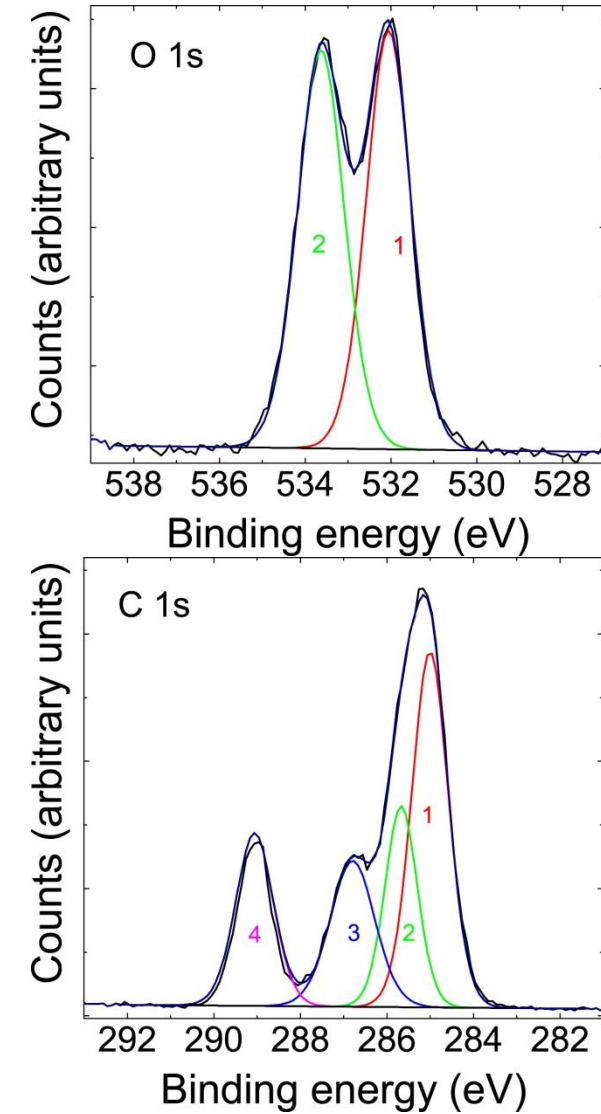
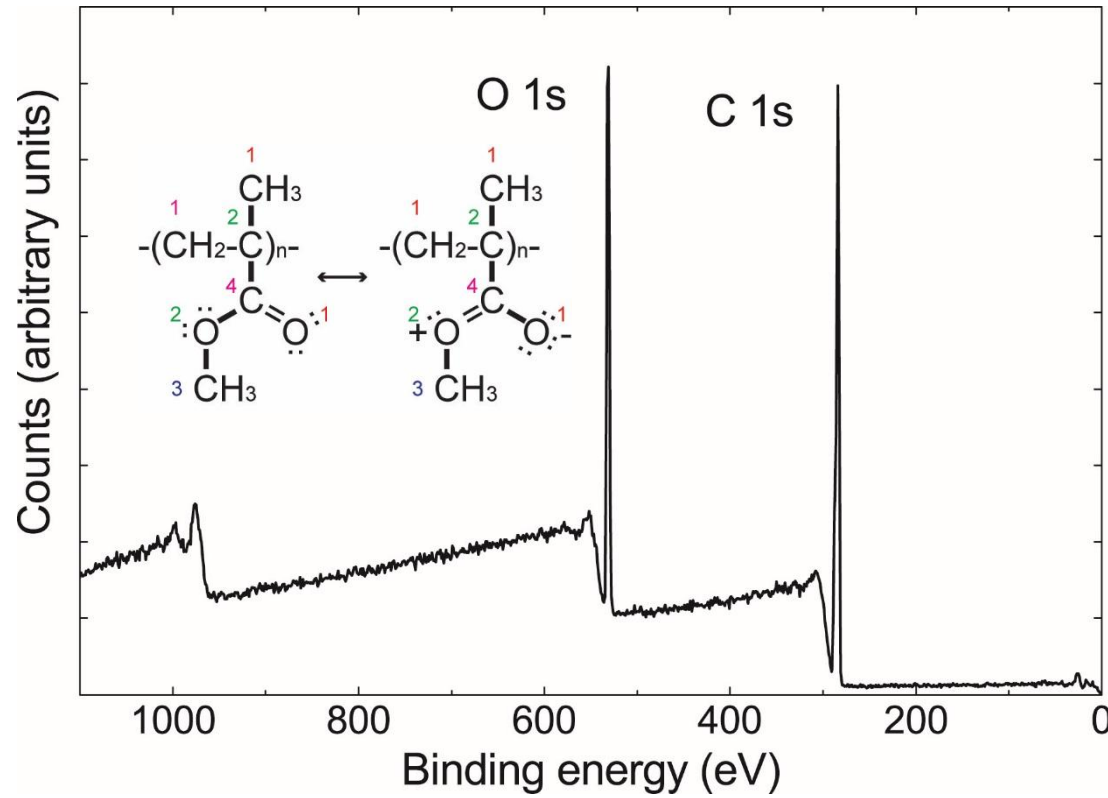


13 IIIA 3A	14 IVA 4A	15 VA 5A	16 VIA 6A	17 VIIA 7A
5 Boron 10.811	6 Carbon 12.011	7 Nitrogen 14.00674	8 Oxygen 15.9994	9 Fluorine 18.998403

Functional Group	C 1s Binding Energy
hydrocarbon	C-H, C-C
amine	C-N
alcohol, ether	C-O-H, C-O-C
Cl bound to C	C-Cl
F bound to C	C-F
carbonyl	C=O

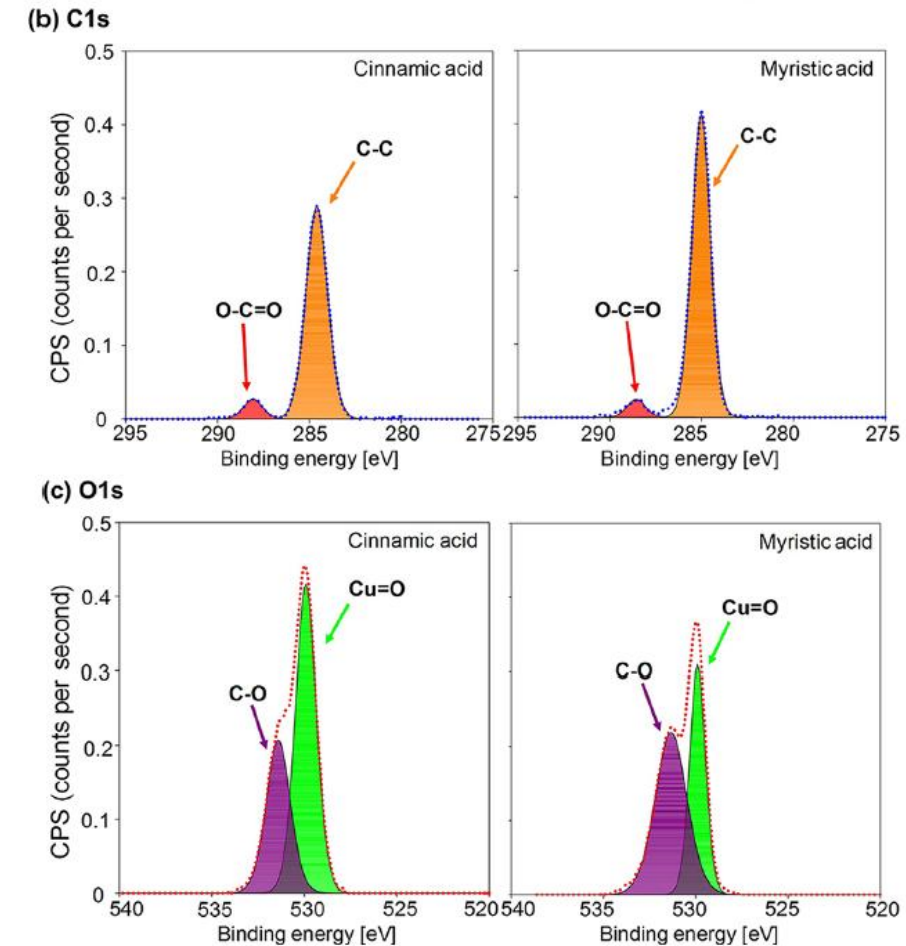
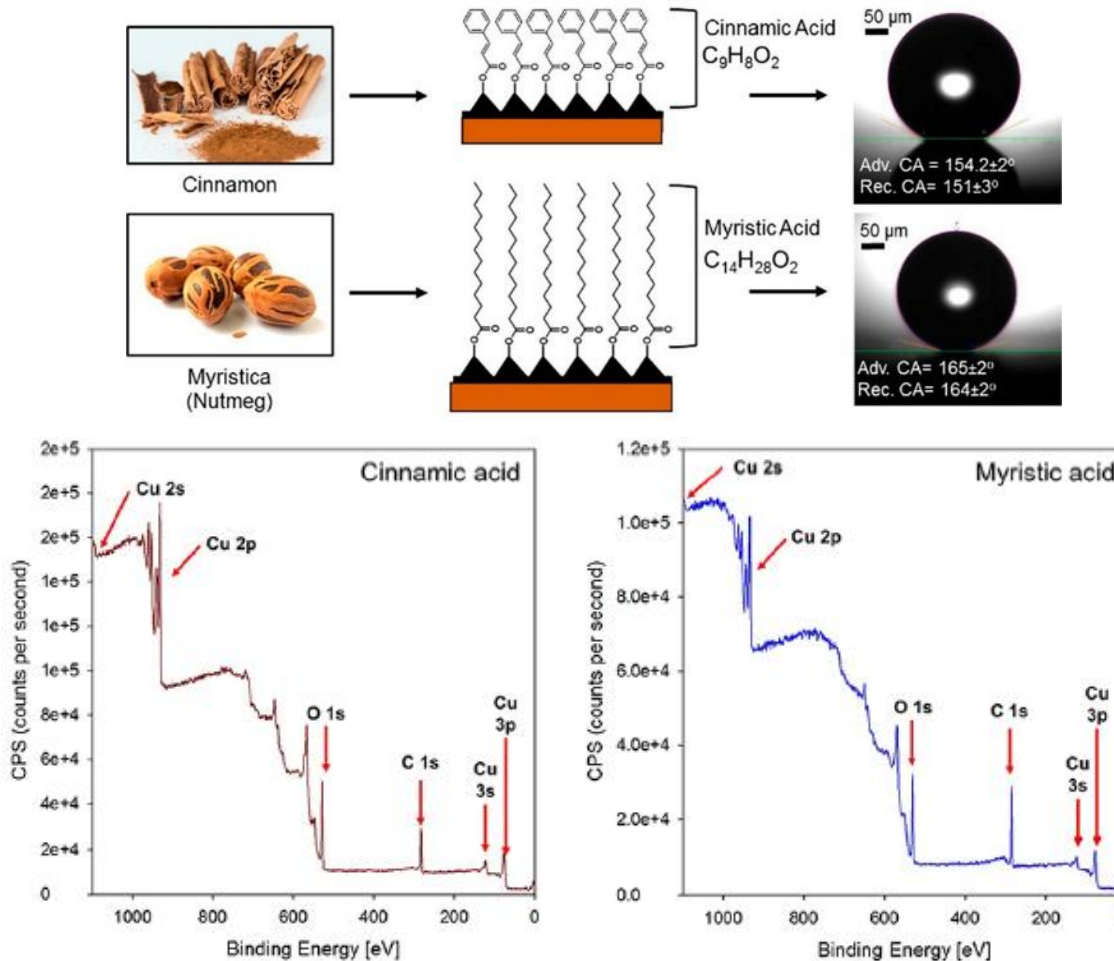
# Chemical Shifts

## XPS of polymethylmethacrylate



# Superhydrophobic Materials

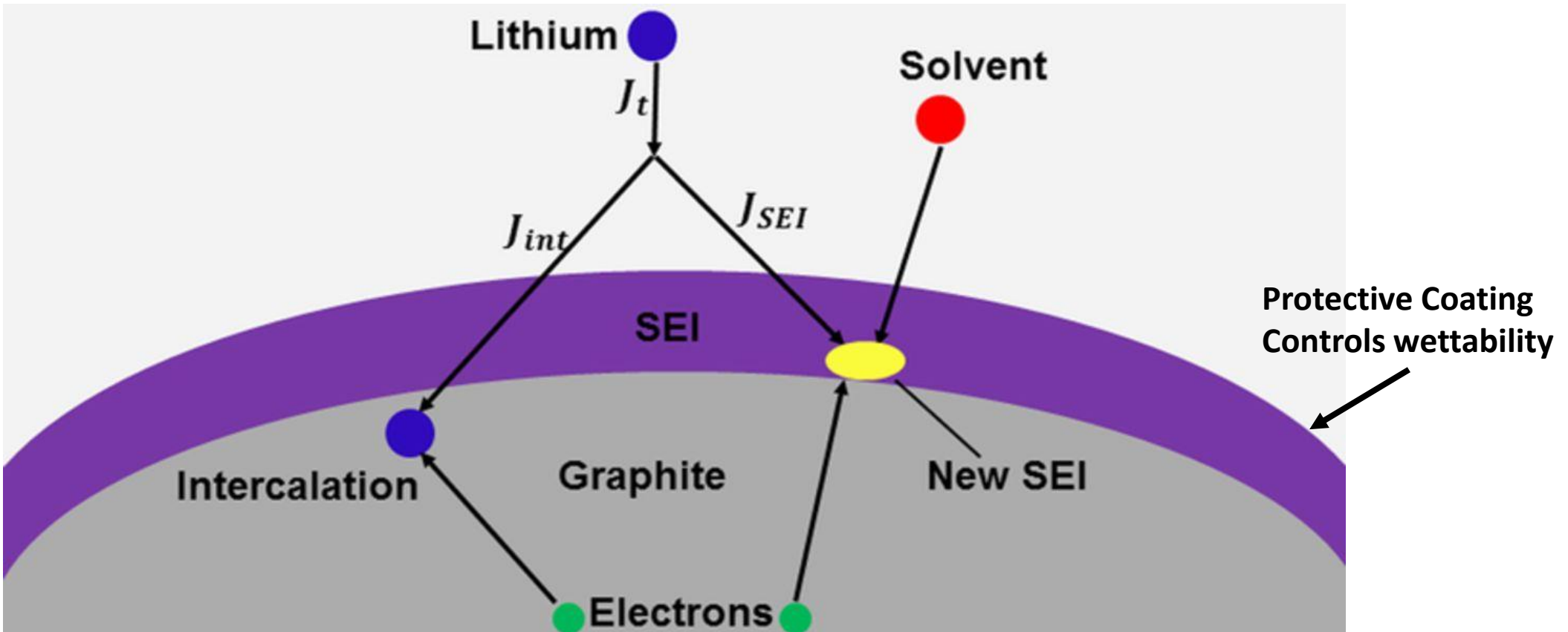
## Superhydrophobic Surfaces from Naturally Derived Hydrophobic Materials



S. M. R. Razavi, J. Oh, S. Sett, L. Feng, X. Yan, M. J. Hoque, A. Liu, R. T. Haasch, M. Masoomi, R. Bagheri, N. Miljkovic, "Superhydrophobic Surfaces Made From Naturally Derived Hydrophobic Materials," *ACS Sustainable Chem. Eng.*, 5(12), 11362 (2017). [doi:10.1021/acssuschemeng.7b02424](https://doi.org/10.1021/acssuschemeng.7b02424).

# Solid Electrolyte Interphase (SEI)

Parallel pathways for the transport and intercalation of Li ions into an active particle and the growth of the SEI layer through degradation reactions of solvent molecules with Li ions.

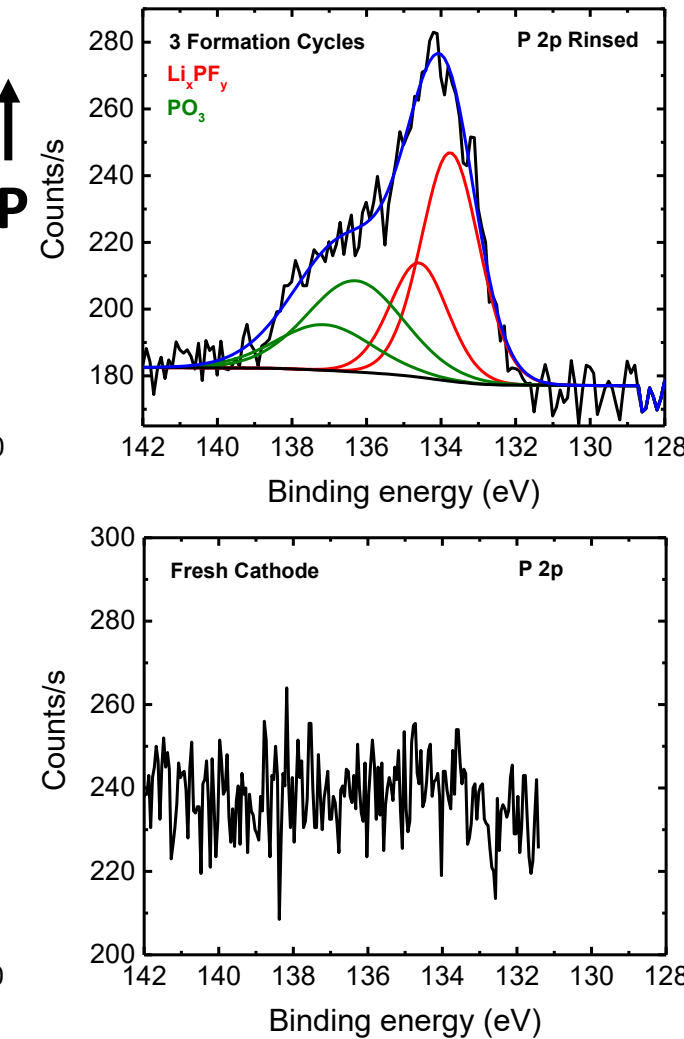
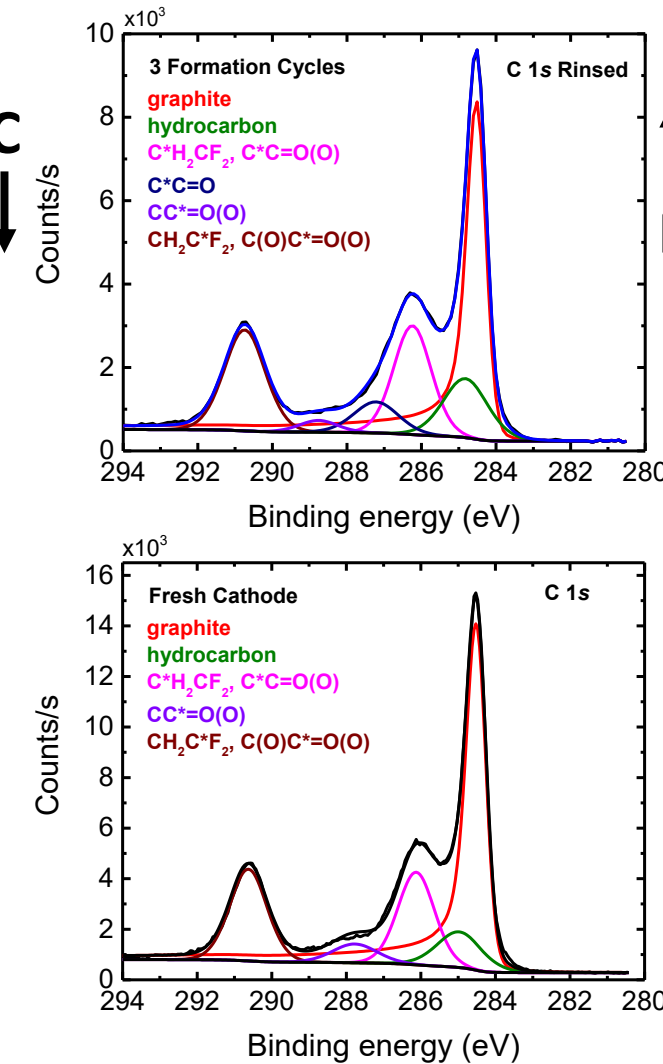
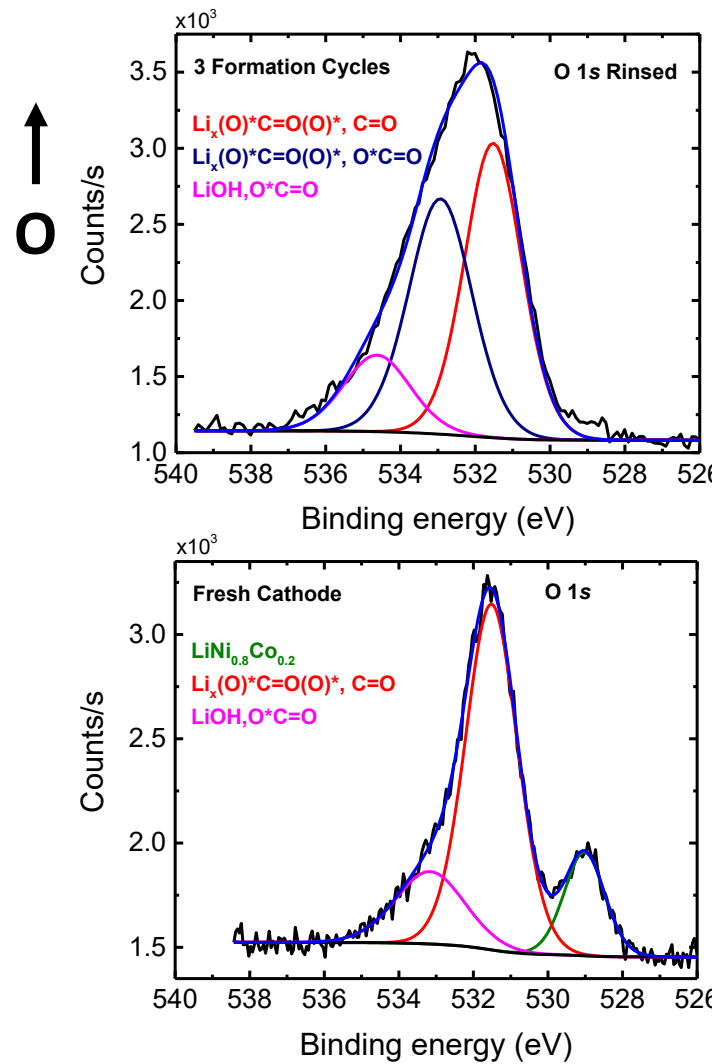


A. A. Tahmasbi et al. J. Electrochem. Soc. 2017;164:A1307-A1313

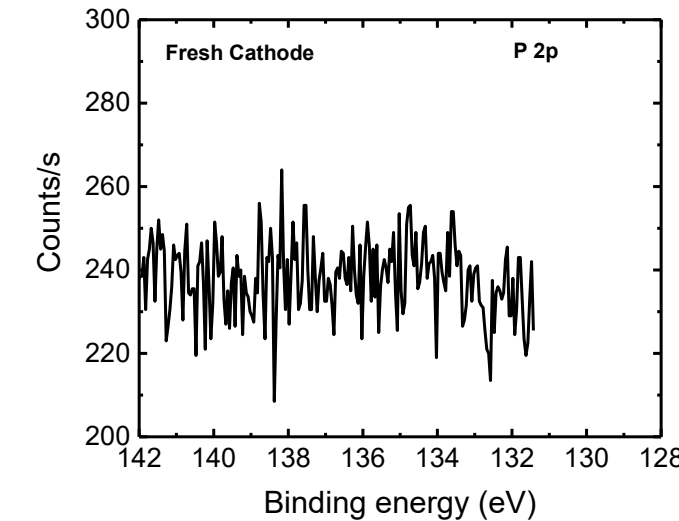
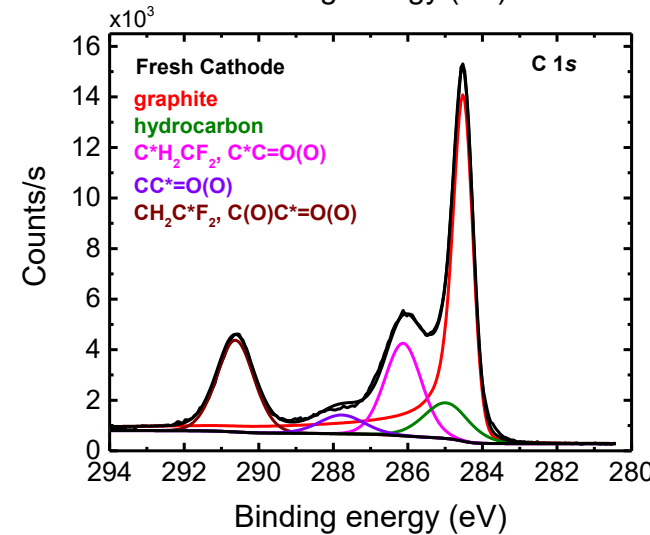
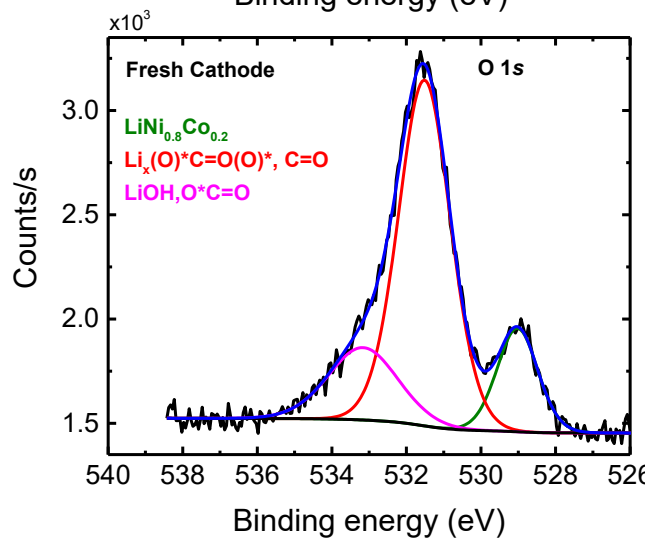
Journal of The Electrochemical Society

©2017 by The Electrochemical Society

# Cathode (positive electrode)- $\text{LiNi}_{0.8}\text{Co}_{0.2}\text{O}_2$



**3 Formation Cycles**



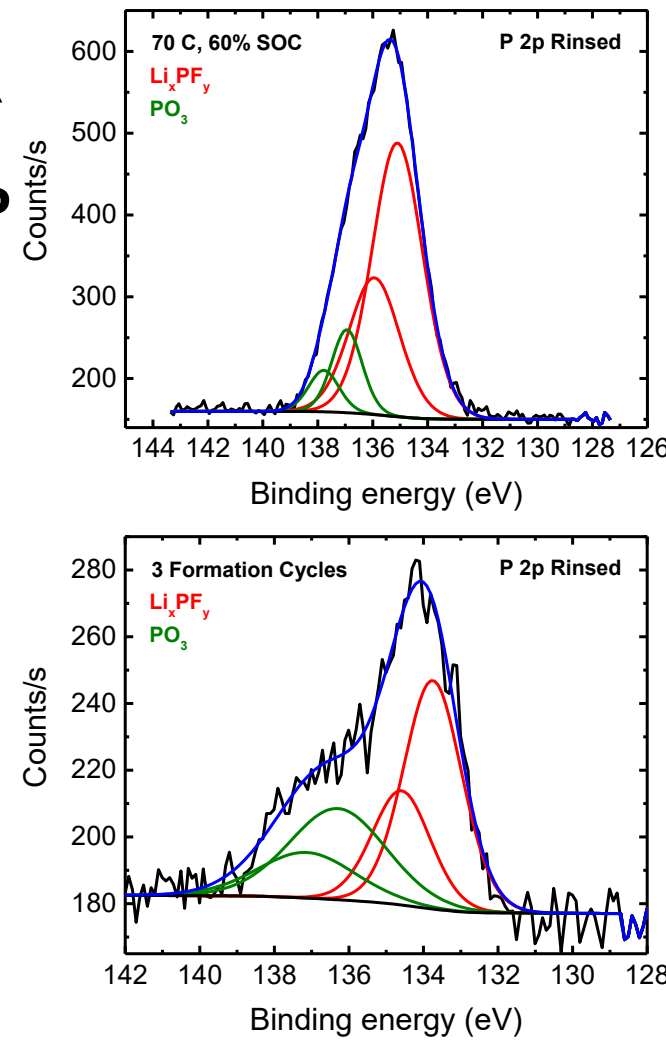
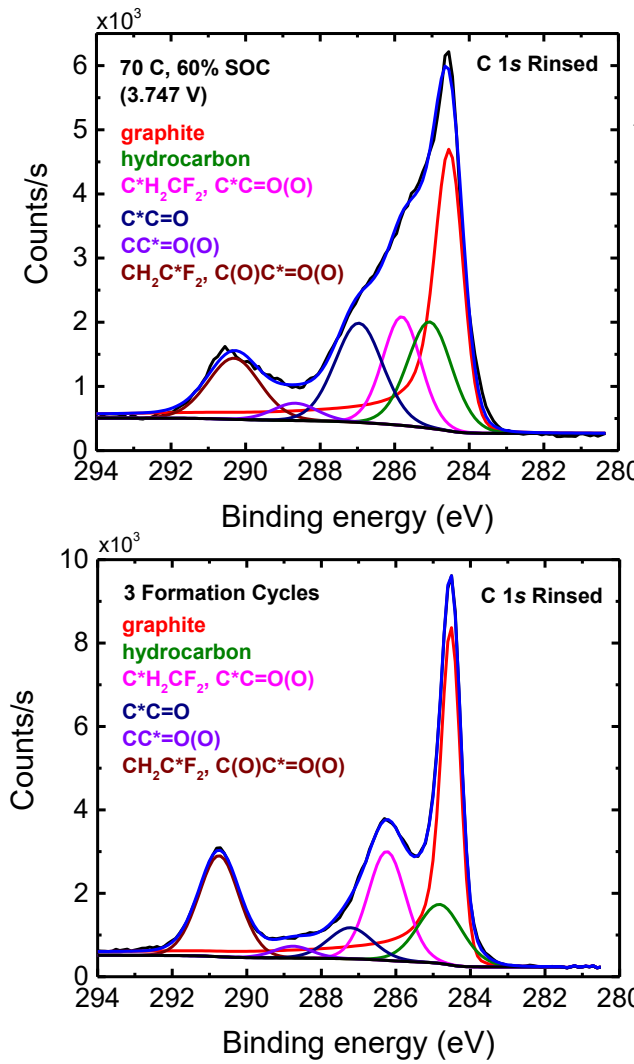
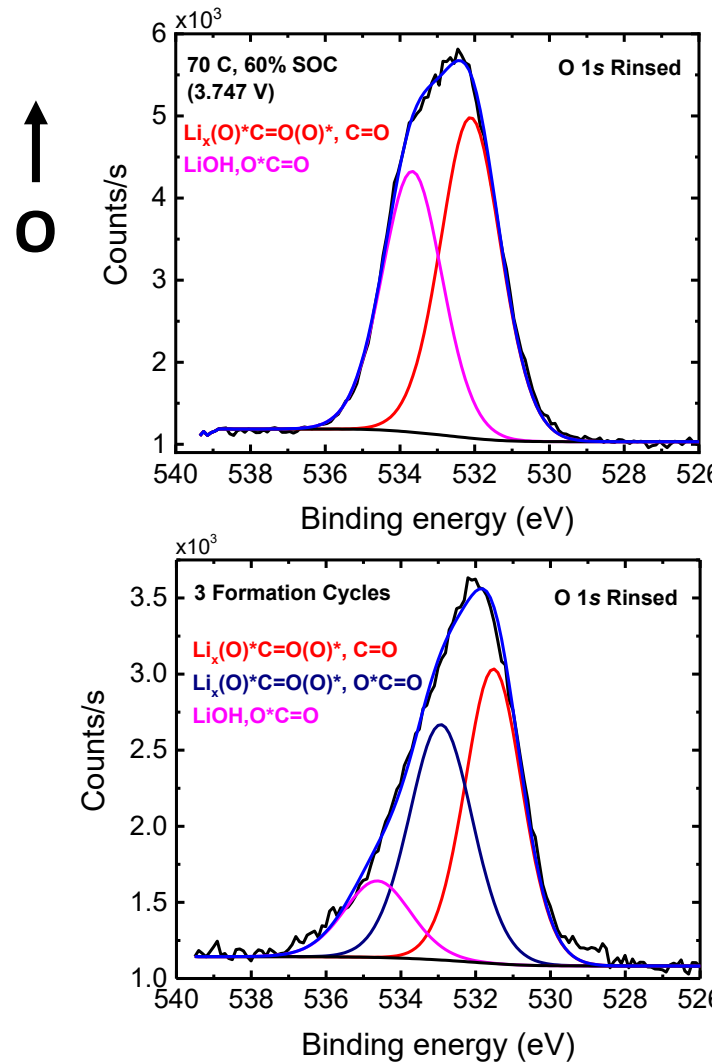
**Fresh**



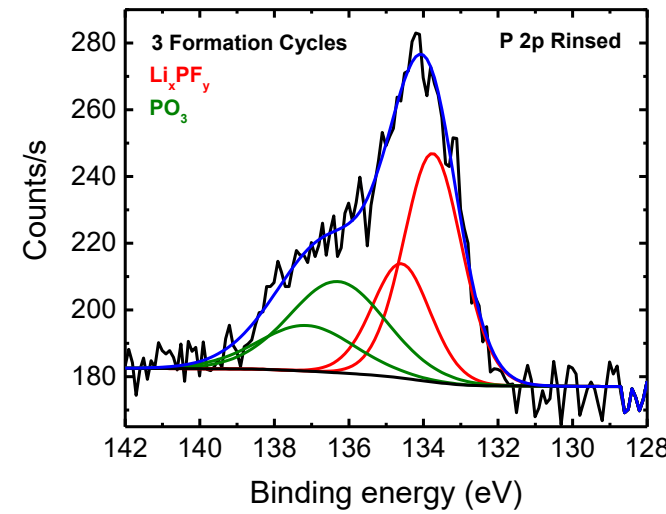
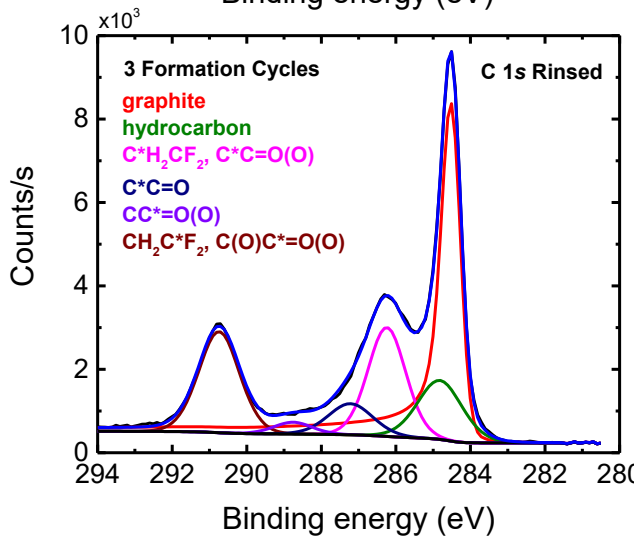
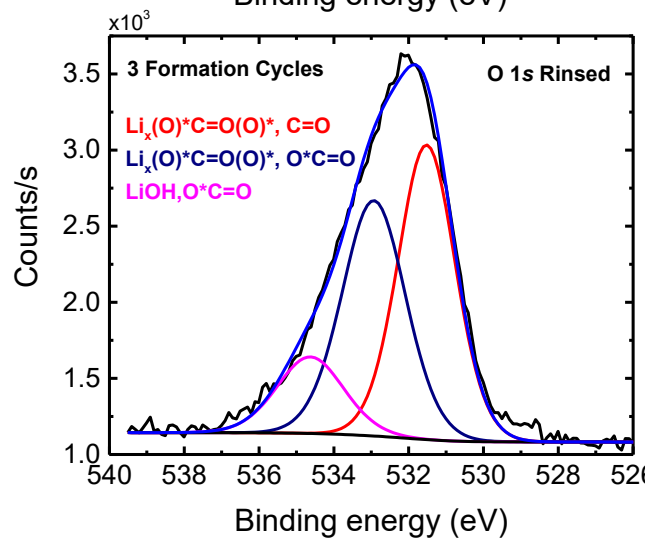
D. P. Abraham, J. Liu, C. H. Chen, Y. E. Hyung, M. Stoll, N. Elsen, S. McLaren, R. Twisten, R. Haasch, E. Sammann I. Petrov, K. Amine, G. Henriksen, "Diagnosis of power fade mechanisms in high-power lithium-ion cells," *J. Power Sources*, **119-121**, 511-516 (2003).

R. T. Haasch, D. P. Abraham, " $\text{LiNi}_{0.8}\text{Co}_{0.2}\text{O}_2$ -based high-power lithium-ion battery positive electrodes analyzed by X-ray photoelectron spectroscopy," *Surface Science Spectra*, **23**, 112-172 (2016).

# Cathode (positive electrode)- $\text{LiNi}_{0.8}\text{Co}_{0.2}\text{O}_2$



70 °C,  
60% SOC



3 Formation  
Cycles

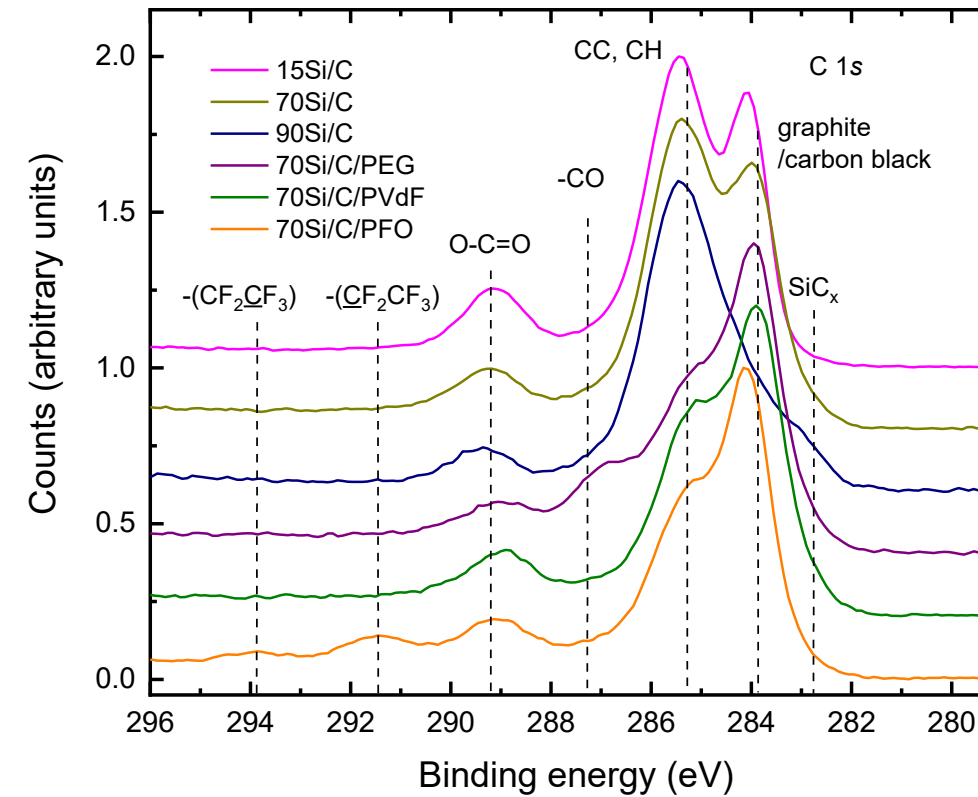
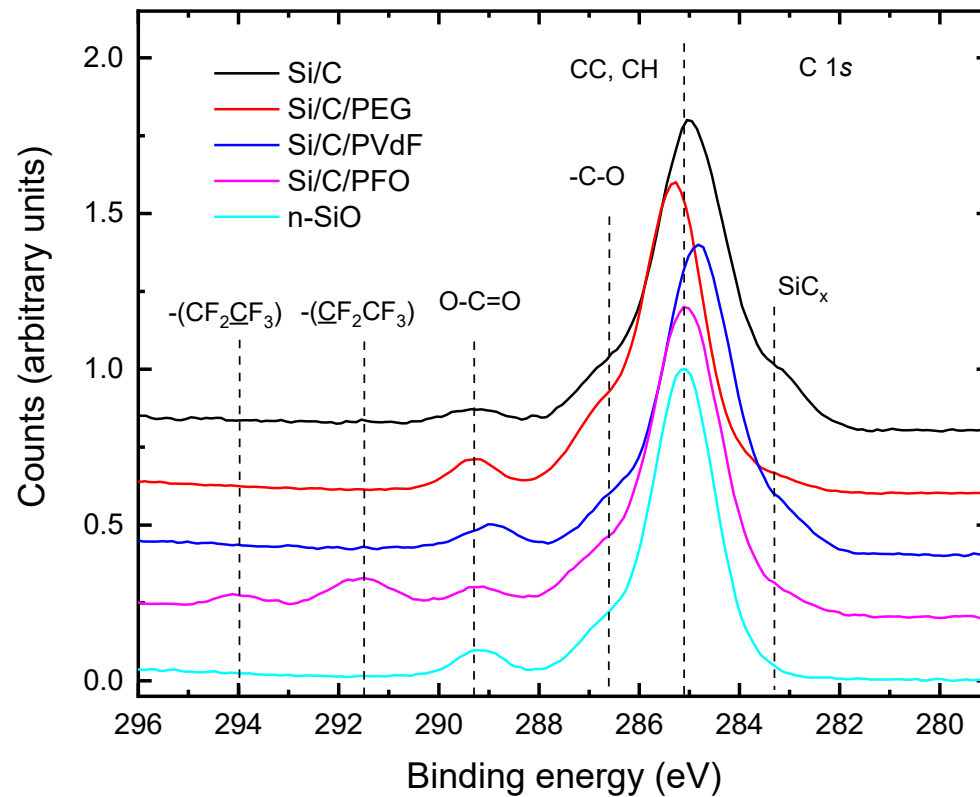
D. P. Abraham, J. Liu, C. H. Chen, Y. E. Hyung, M. Stoll, N. Elsen, S. MacLaren, R. Twisten, R. Haasch, E. Sammann I. Petrov, K. Amine, G. Henriksen, "Diagnosis of power fade mechanisms in high-power lithium-ion cells," *J. Power Sources*, **119-121**, 511-516 (2003).

R. T. Haasch, D. P. Abraham, " $\text{LiNi}_{0.8}\text{Co}_{0.2}\text{O}_2$ -based high-power lithium-ion battery positive electrodes analyzed by X-ray photoelectron spectroscopy," *Surface Science Spectra*, **23**, 112-172 (2016).

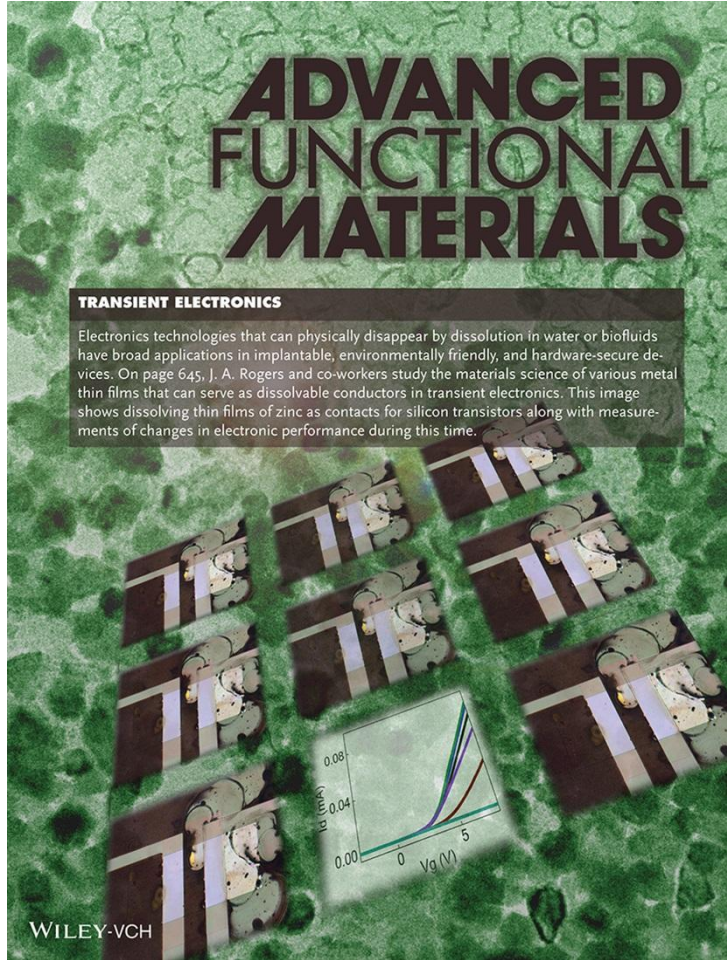


# Anode (negative electrode)- Si Based Materials

## Si powders and electrodes for high-energy lithium-ion cells

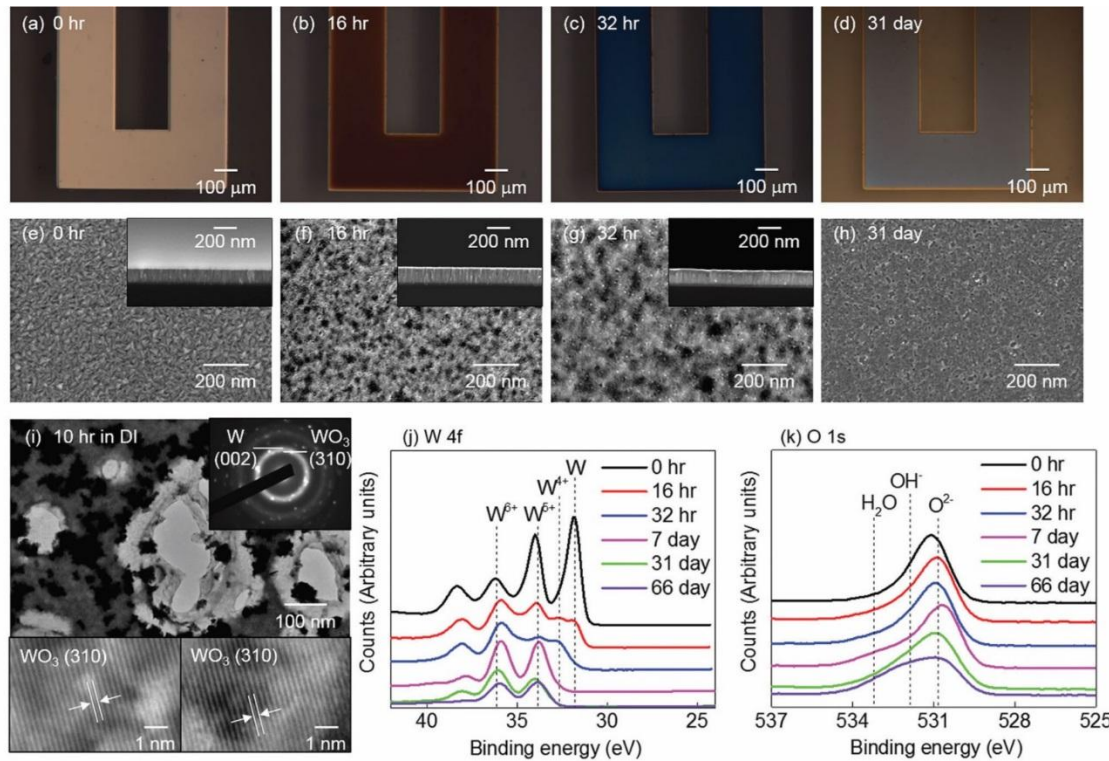


# Dissolvable Metals



## Dissolvable Metals for Transient Electronics

Lan Yin, Huanyu Cheng, Shimin Mao, Richard Haasch, Yuhao Liu, Xu Xie, Suk-Won Hwang, Harshvardhan Jain, Seung-Kyun Kang, Yewang Su, Rui Li, Yonggang Huang, and John A. Rogers\*



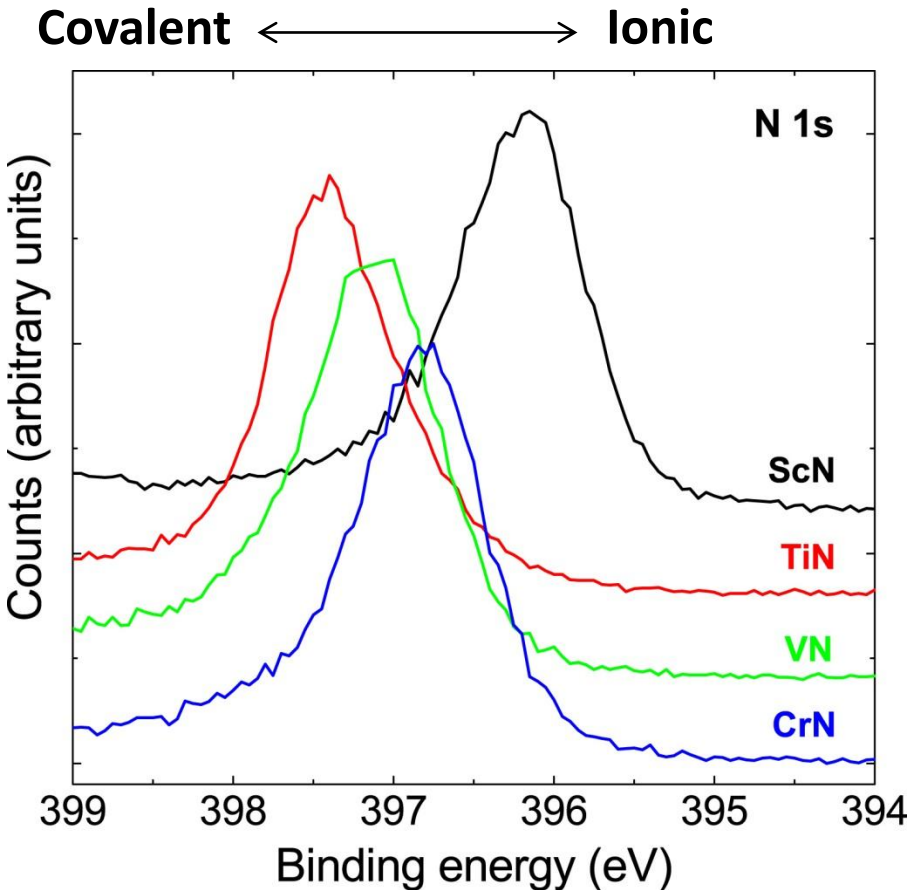
L. Yin, H. Cheng, S. Mao, R. Haasch, Y. Liu, X. Xie, S.-W. Hwang, H. Jain, S.-K. Kang, Y. Su, R. Li, Y. Huang, J. A. Rogers, "Dissolvable Metals for Transient Electronics," *Adv. Funct. Mater.*, **24**, 645 (2014).

# Transition Metal Nitrides

## N 1s spectra of First-Row Transition Metal Nitrides: ScN, TiN, VN, and CrN

p-d hybridization 8 MO's

	Anti-bonding e <sup>-</sup> /Formula Unit (nominal)	Binding Energy, eV
ScN	-0.17 (0)	396.1
TiN	1 (1)	397.3
VN	1.9 (2)	397.0
CrN	2.9 (3)	396.7

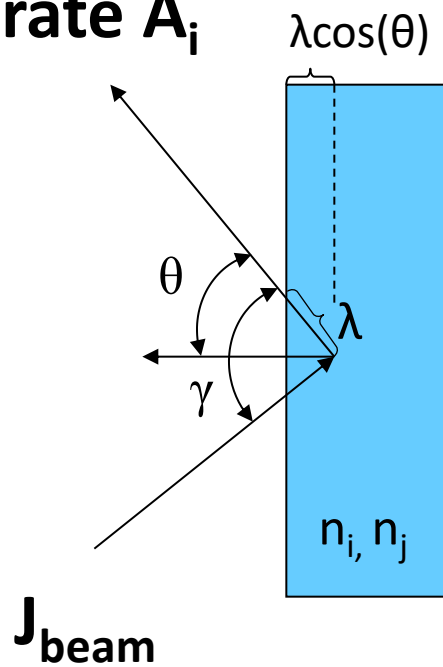


R. T. Haasch, T.-Y. Lee, D. Gall, C.-S. Shin, J. E. Greene, I. Petrov, *Surf. Sci. Spectra*, **7**, 169 (2000), *Surf. Sci. Spectra*, **7**, 193 (2000), *Surf. Sci. Spectra*, **7**, 221 (2000), *Surf. Sci. Spectra*, **7**, 250 (2000).

# Quantitative Surface Analysis: XPS

**detector count**

**rate  $A_i$**



**Assuming a Homogeneous sample:**

$A_i$  = detector count rate

$$A_i = (\text{electrons/volume})(\text{volume})$$

$$A_i = (N_i \sigma_i(\gamma) J T(E_i)) (a \lambda_i(E_i) \cos \theta)$$

**Sample Dependent Terms**

where:  $N$  = atoms/cm<sup>3</sup>

$\sigma(\gamma)$  = photoelectric (scattering) cross-section, cm<sup>2</sup>

$\lambda(E_i)$  = inelastic electron mean-free path, cm

**Instrument Dependent Terms**

$J$  = X-ray flux, photon/cm<sup>2</sup>-sec

$T(E_i)$  = analyzer transmission function

$a$  = analysis area, cm<sup>2</sup>

$\theta$  = photoelectron emission angle

# Quantitative Surface Analysis: XPS

**By assuming the concentration to be a relative ratio of atoms, we can neglect the terms that depend only on the instrument:**

$$N_i = A_i / \sigma_i T(E_i) \lambda_i(E_i)$$

It is difficult to accurately determine  $\lambda_i$  so it is usually neglected. Modern acquisition and analysis software can account for the transmission function.

$$N_i = A_i / S_i$$

$$C_i = A_i / S_i / \sum A_{i,j} / S_{i,j}$$

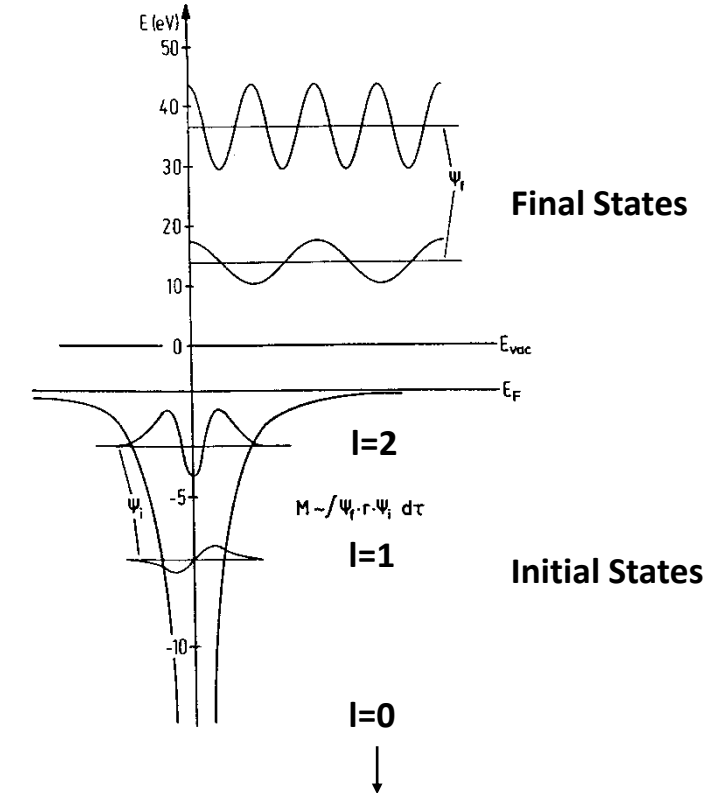
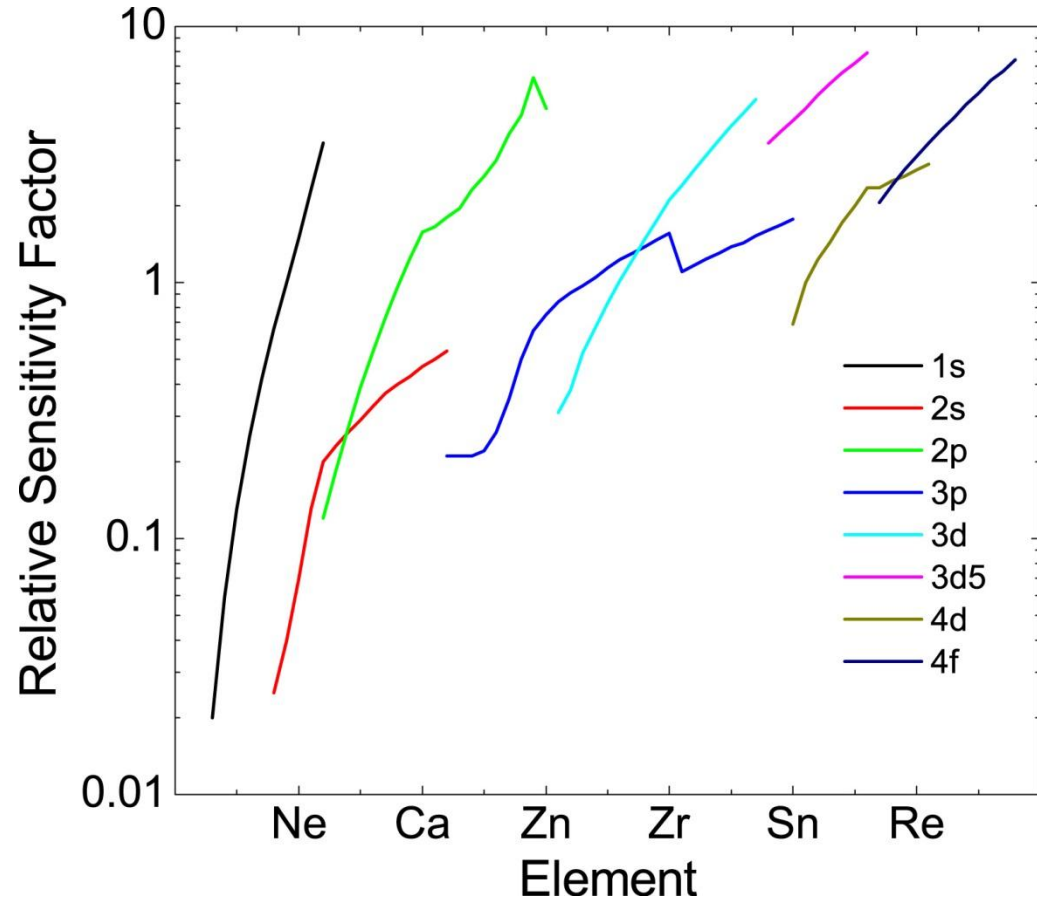
The values of S are determined theoretically or empirically with standards.

**XPS is considered to be a *semi-quantitative technique*.**



# Quantitative Surface Analysis: XPS

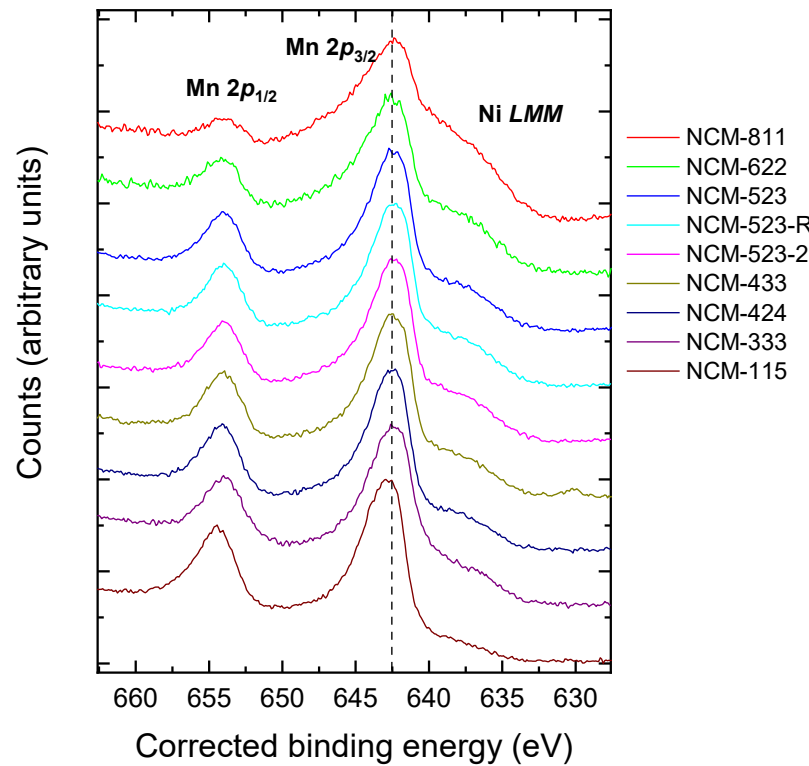
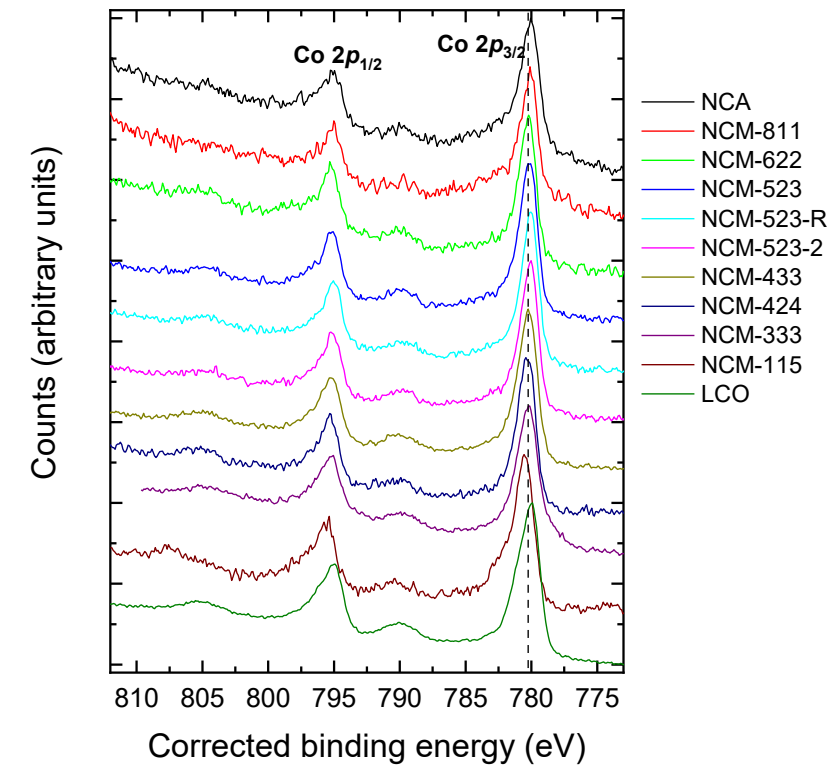
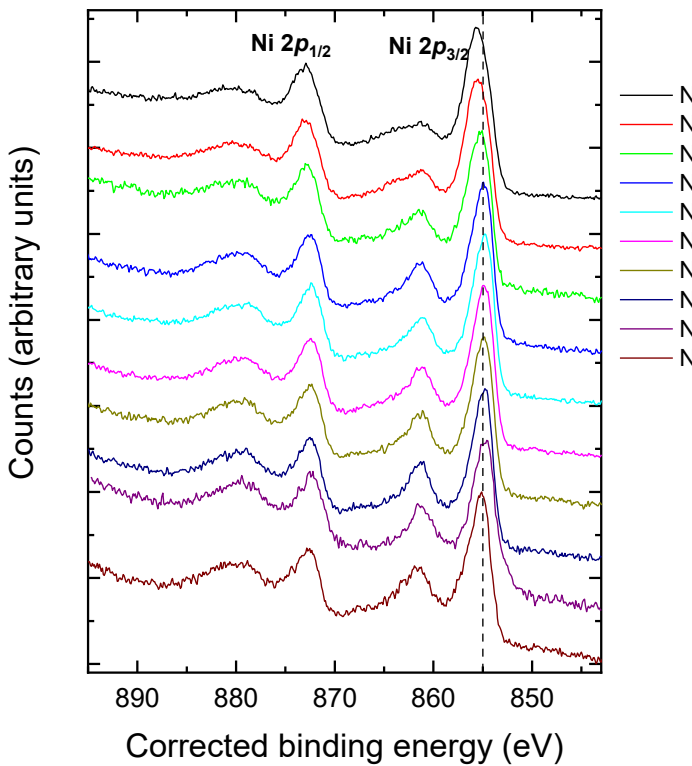
## XPS Relative Elemental Sensitivities



S. Hüfner, *Photoelectron Spectroscopy Principles and Applications*, Second Edition, (Springer, Berlin Heidelberg, 1996). ISBN 3-540-60875-3.

# NCM Family of Oxide Materials - Raw Powder

## Lithium-bearing Oxides for Rechargeable Li-ion Batteries: $\text{NCM}_{xyz} (\text{LiNi}_{x/10}\text{Co}_{y/10}\text{Mn}_{z/10}\text{O}_2, \text{with } x+y+z=10)$

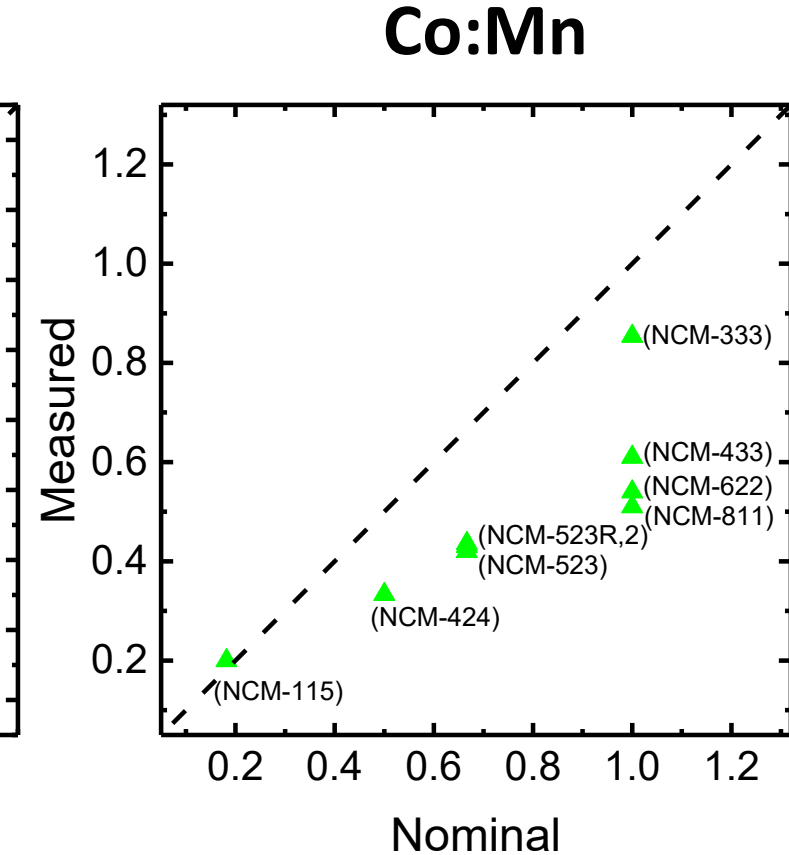
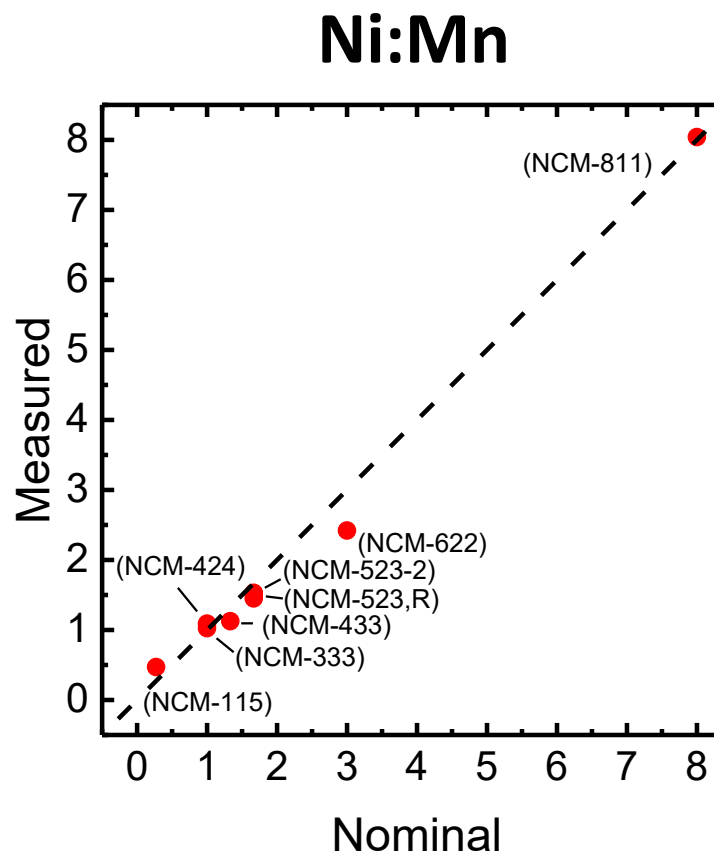
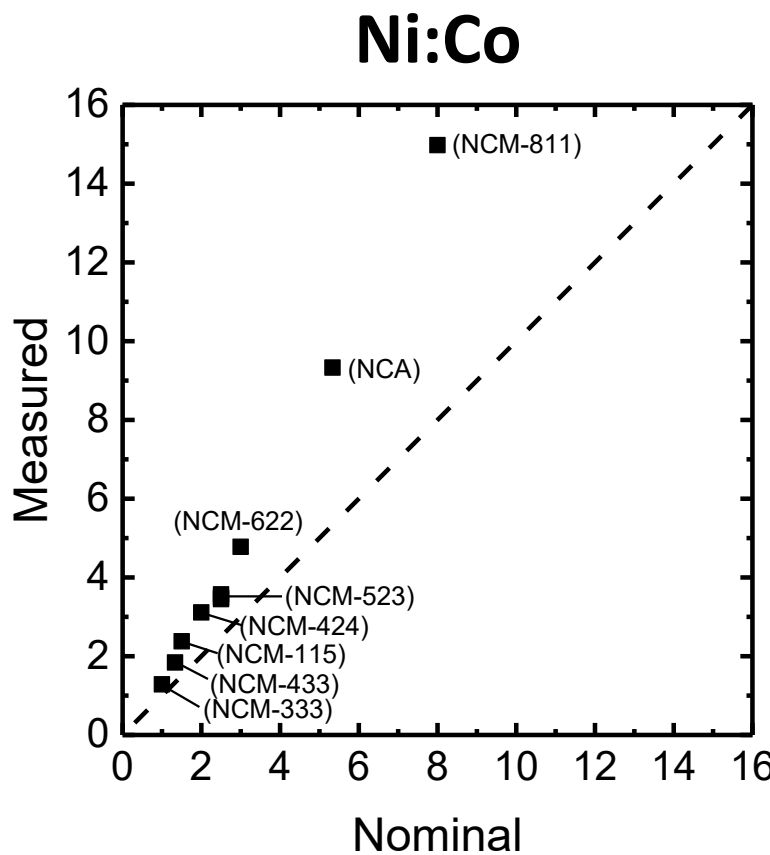


I

R. T. Haasch, S. E. Trask, D. P. Abraham, "Lithium-bearing oxides for rechargeable Li-ion batteries," *Surf. Sci. Spectra*, **26**, 014002 (2019). [doi:10.1116/1.5080232](https://doi.org/10.1116/1.5080232).

# NCM Family of Oxide Materials - Raw Powder

Lithium-bearing Oxides for Rechargeable Li-ion Batteries:  
 $\text{NCM}_{xyz} (\text{LiNi}_{x/10}\text{Co}_{y/10}\text{Mn}_{z/10}\text{O}_2, \text{with } x+y+z=10)$



# Transition Metal Nitrides

## First-Row Transition Metal Nitrides: ScN, TiN, VN, and CrN

XPS Analysis			ScN	TiN	VN	CrN
Binding energy (eV)	Metal 2p <sub>3/2</sub>	Major peak	400.4	455.1	513.2	574.4
	Metal 2p <sub>1/2</sub>	Satellite <sup>a</sup>		457.9	515.5	575.5
		Major peak	404.9	461.0	520.7	584.0
		Satellite <sup>a</sup>		463.8	523.0	585.1
N 1s		396.1	397.3	397.0	396.7	
Composition (N/metal)	As Deposited	1.13	1.00	1.02	0.73 <sup>b</sup>	
	After ion bombardment	0.99	0.73	0.46	0.55 <sup>b</sup>	
Bulk value from RBS		1.11±0.03	1.02±0.02	1.06±0.02	1.04±0.02	

- a. The satellite is due to a transition into a relaxed final state
- b. The composition determination of the CrN layers by peak fitting is less reliable because the commonly used Shirley method for background subtraction does not accurately describe the experimental data.

### Nitrogen/Metal peak ratio decreases after sputtering



R. T. Haasch, T.-Y. Lee, D. Gall, C.-S. Shin, J. E. Greene, I. Petrov, *Surf. Sci. Spectra*, **7**, 169 (2000), *Surf. Sci. Spectra*, **7**, 193 (2000), *Surf. Sci. Spectra*, **7**, 221 (2000), *Surf. Sci. Spectra*, **7**, 250 (2000).

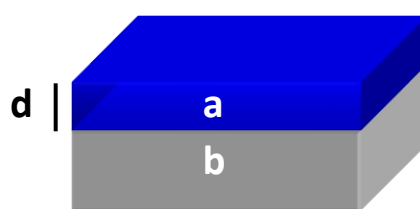
# Layer Thickness Measurement

## Layer thickness calculation: Two-Layer Model

Assuming only inelastic scattering

Beer-Lambert relationship:

$$I = I_0 \exp(-d/\lambda \cos\theta)$$

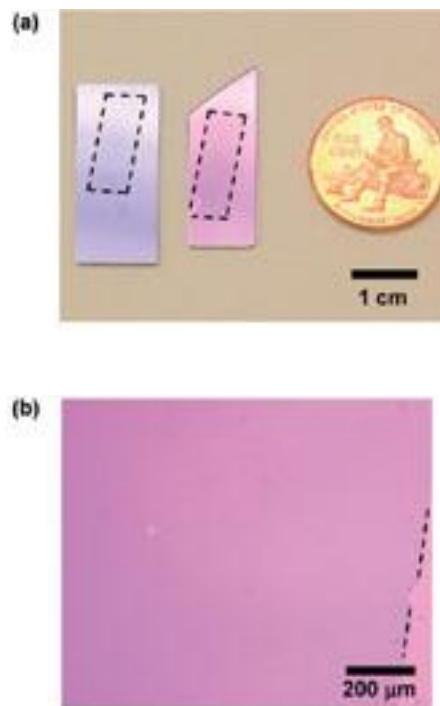
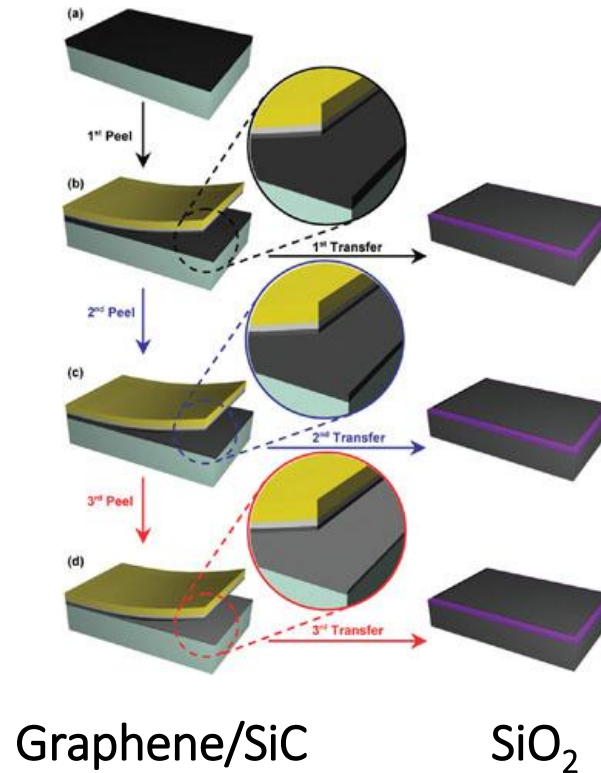

$$\frac{I_a}{I_b} \rightarrow \ln \left( \frac{N_a n_b \rho_b \lambda_b M W_a}{N_b n_a \rho_a \lambda_a M W_b} + 1 \right) = \frac{d}{\lambda_a \cos \theta}$$

Where:  $\eta$  = number of atoms per molecule unit,  
 $\rho$  = molecular density,  
 $\lambda$  = inelastic mean-free path,  
MW = molecular weight,  
N = atomic concentration.

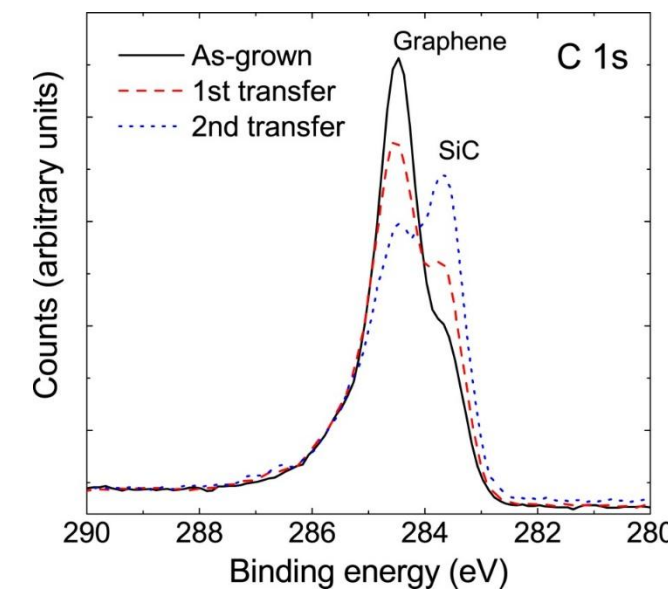


# Graphene Transfer

## Layer-by-Layer Transfer of Multiple, Large Area Sheets of Graphene Grown in Multilayer Stacks on a Single SiC Wafer



	Thickness, nm
As-grown	2.0
1 <sup>st</sup> Transfer	1.5
2 <sup>nd</sup> Transfer	0.8

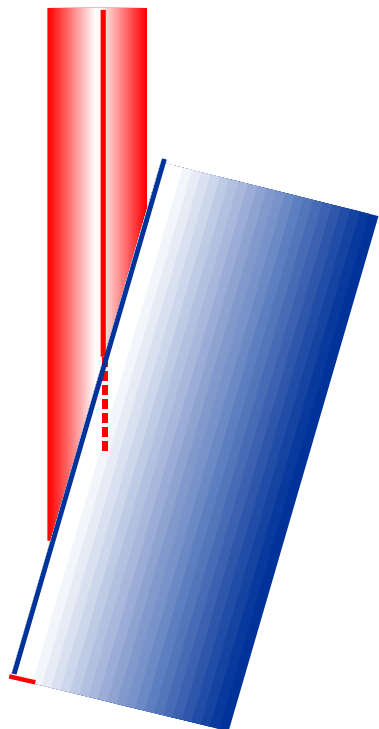


S. Unarunotai, J. Koepke, C.-L. Tsai, F. Du, C. Chialvo, Y. Murata, R. Haasch, I. Petrov, N. Mason, M. Shim, J. Lyding, J. A. Rogers, *ACS Nano*, **4(10)**, 5591-5598, (2010).

# Angle-resolved XPS

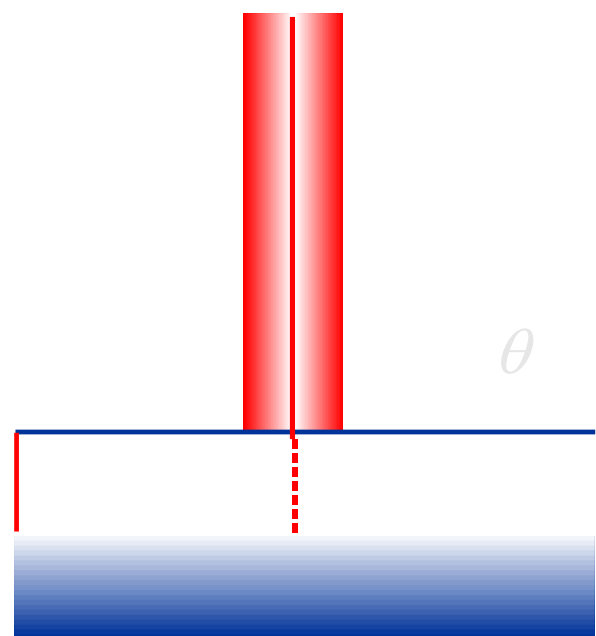
**More Surface Sensitive**

$$\theta = 75^\circ$$

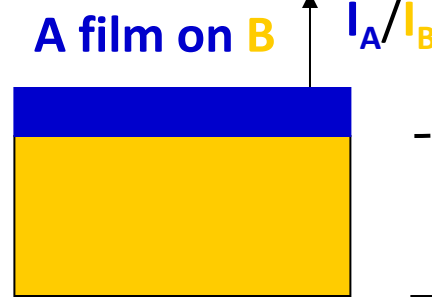


**Less Surface Sensitive**

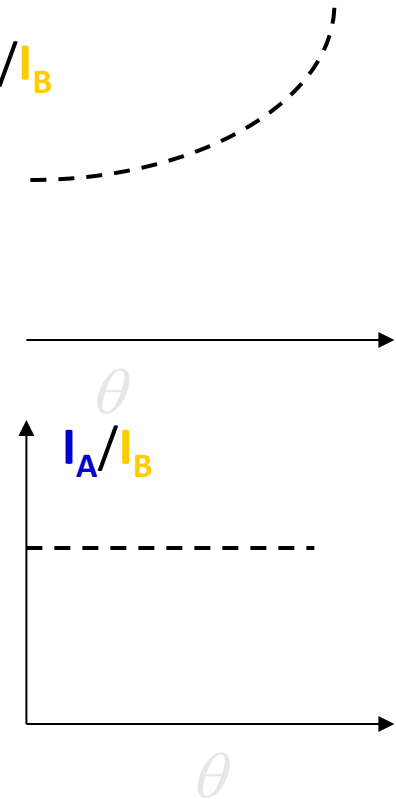
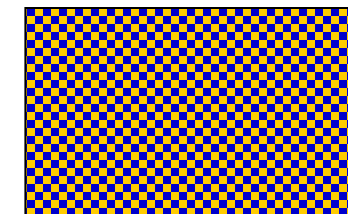
$$\theta = 0^\circ$$



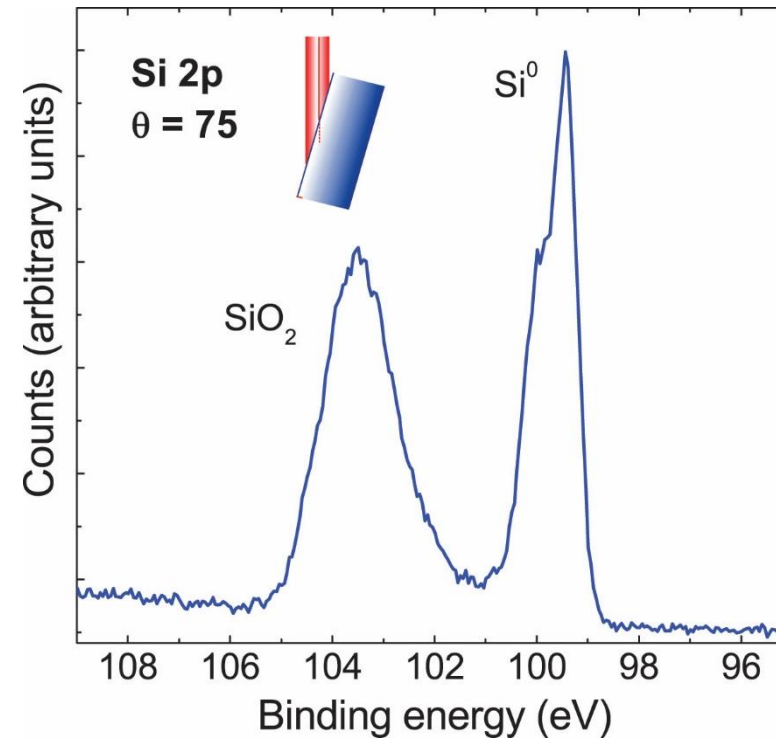
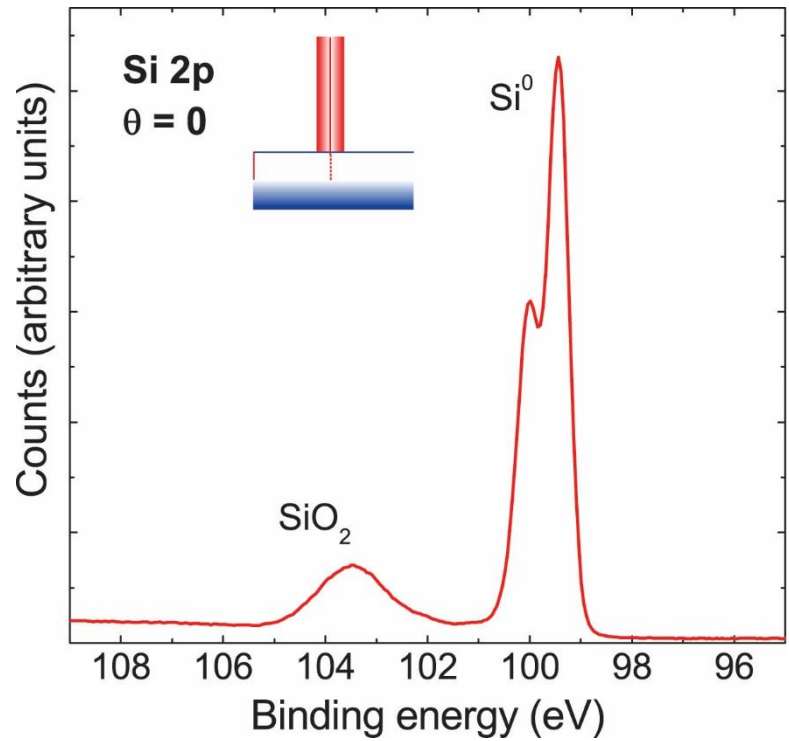
- Information depth =  $d \cos \theta$
- $d$  = Escape depth  $\sim 3 \lambda$
- $\theta$  = Emission angle (relative to surface normal)
- $\lambda$  = Inelastic Mean Free Path



**AB alloy**

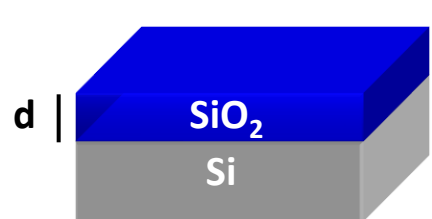


# Angle-resolved XPS - $\text{SiO}_2/\text{Si}$



# Angle-resolved XPS - SiO<sub>2</sub>/Si

## Layer thickness calculation: Angle-resolved XPS

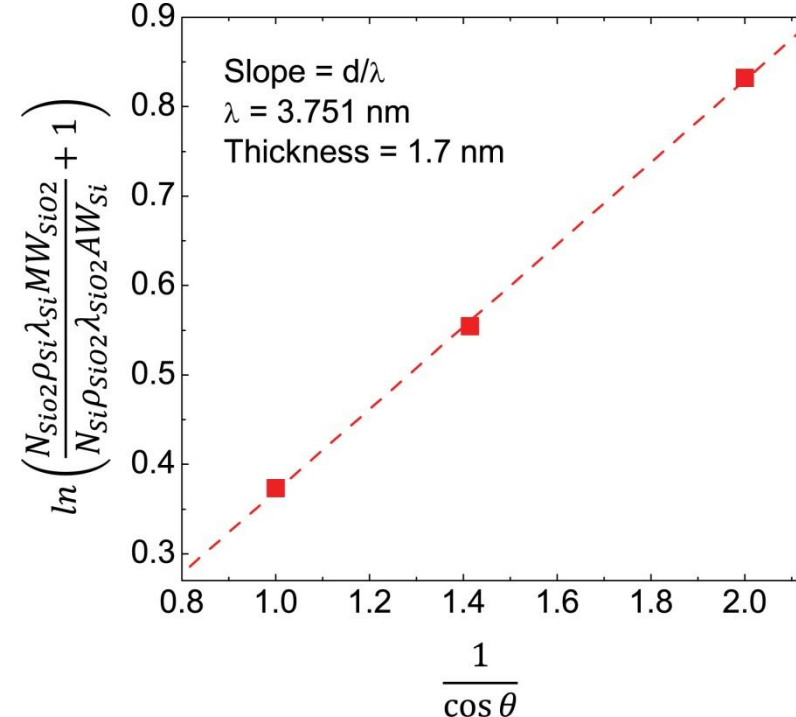


Beer-Lambert relationship:

$$\frac{I_{\text{SiO}_2}}{I_{\text{Si}}} = \ln \left( \frac{N_{\text{SiO}_2} n_{\text{Si}} \rho_{\text{Si}} \lambda_{\text{Si}} M W_{\text{SiO}_2}}{N_{\text{Si}} n_{\text{SiO}_2} \rho_{\text{SiO}_2} \lambda_{\text{SiO}_2} M W_{\text{Si}}} + 1 \right) = \frac{d}{\lambda_{\text{SiO}_2} \cos \theta}$$

Plot:

$$\ln \left( \frac{N_{\text{SiO}_2} n_{\text{Si}} \rho_{\text{Si}} \lambda_{\text{Si}} M W_{\text{SiO}_2}}{N_{\text{Si}} n_{\text{SiO}_2} \rho_{\text{SiO}_2} \lambda_{\text{SiO}_2} M W_{\text{Si}}} + 1 \right) = \frac{d}{\lambda_{\text{SiO}_2} \cos \theta}$$



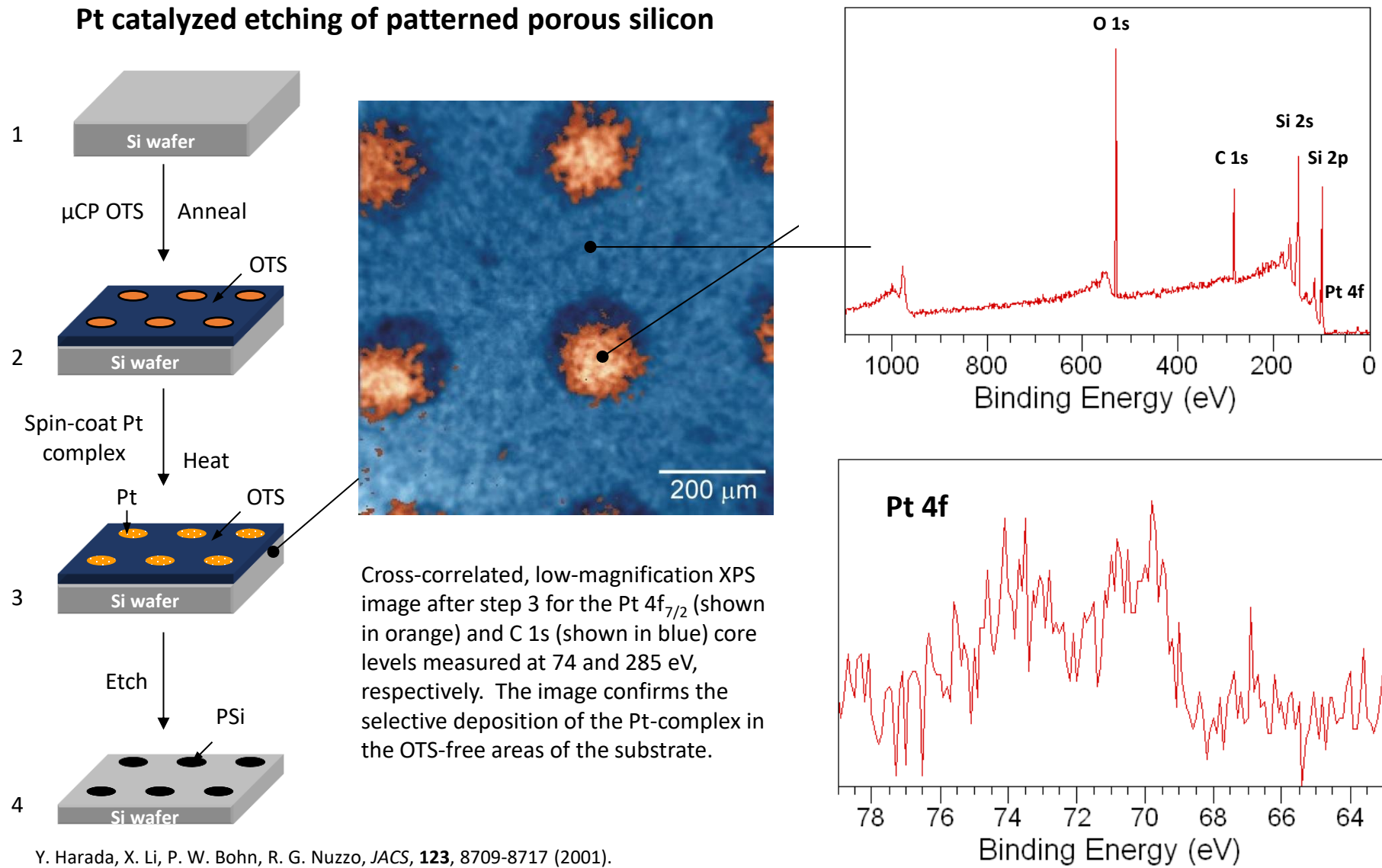
I

R. T. Haasch, "X-ray Photoelectron Spectroscopy (XPS) and Auger Electron Spectroscopy (AES)," in *Practical Materials Characterization*, M. Sardela, ed., (Springer Science + Business Media, New York, 2014). ISBN 978-1-4614-9280-1. doi: 10.1007/978-1-4614-9281-8\_3.

© 2025 University of Illinois Board of Trustees. All rights reserved.

# XPS Imaging: Porous Silicon Pixel Array

I



# XPS Depth Profiling : LIB Solid-state Electrolyte

## Monoatomic ion

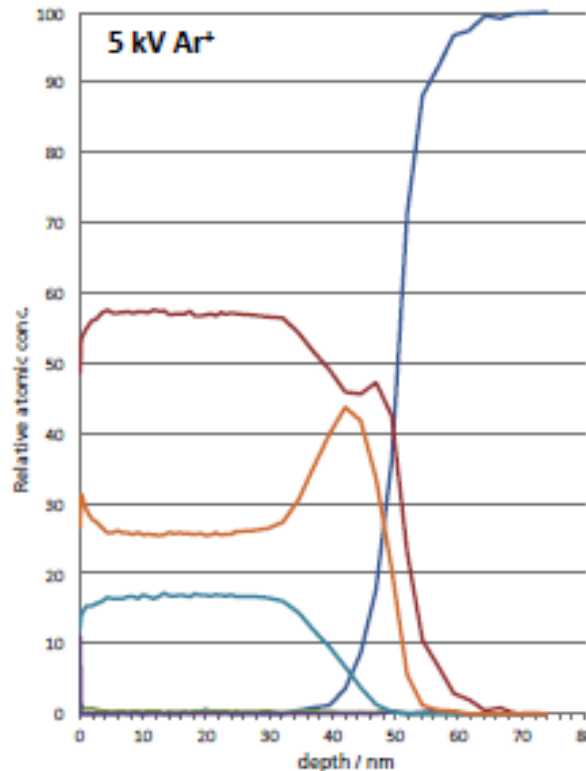


Figure 1(a) Sputter depth profile through ALD LiPON thin film using 5 keV Ar<sup>+</sup>

## Cluster ion

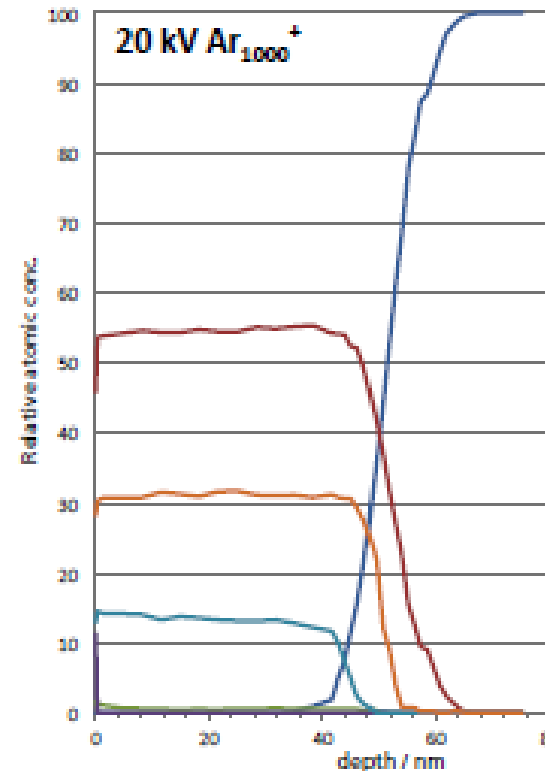


Figure 1(b) Sputter depth profile through ALD LiPON thin film using 20 keV Ar<sub>1000</sub><sup>+</sup>

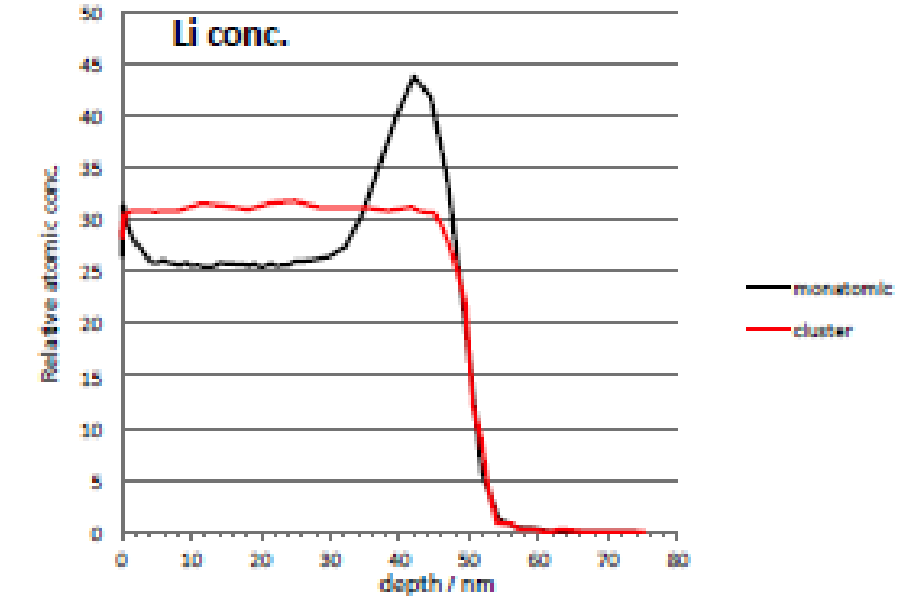
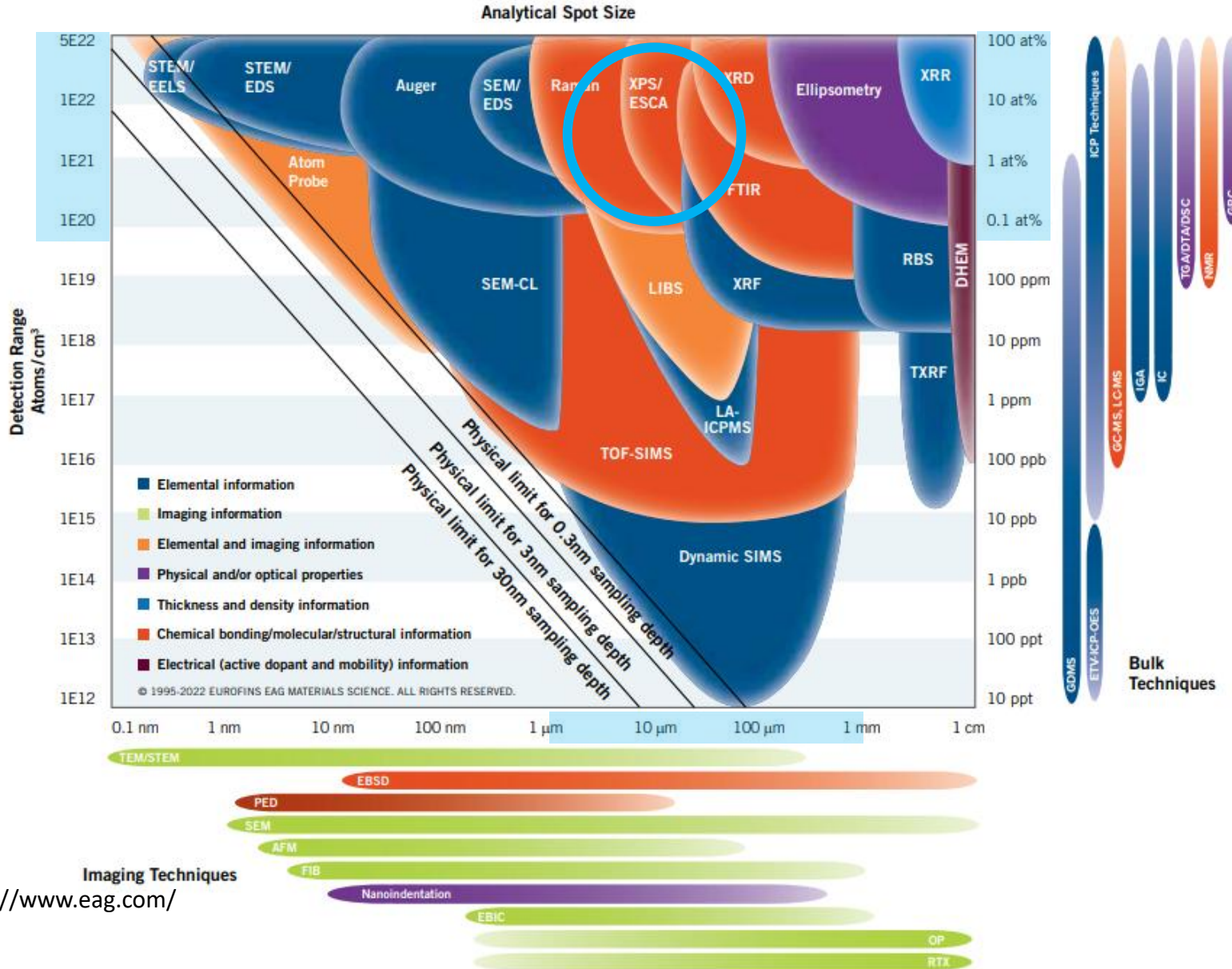


Figure 1(c) comparison of the Li concentration through the same sample generated using monoatomic and cluster ion projectiles.



Image credit: <https://www.kratos.com/>

# Technique Comparison: Resolution vs. Detection Limit



# Technique Comparison: Typical Analysis Depth

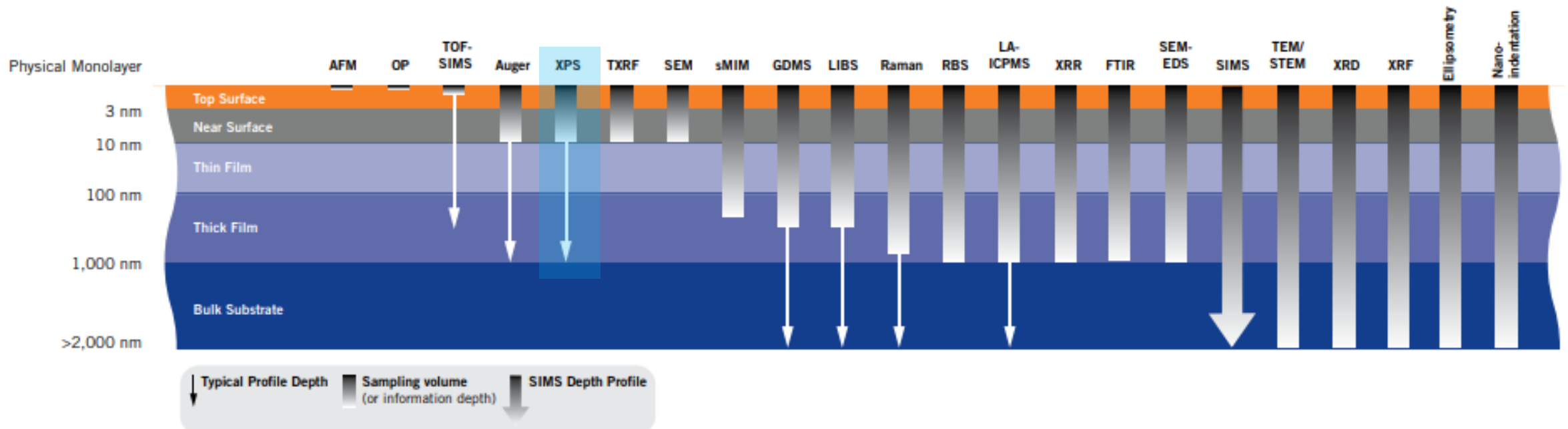
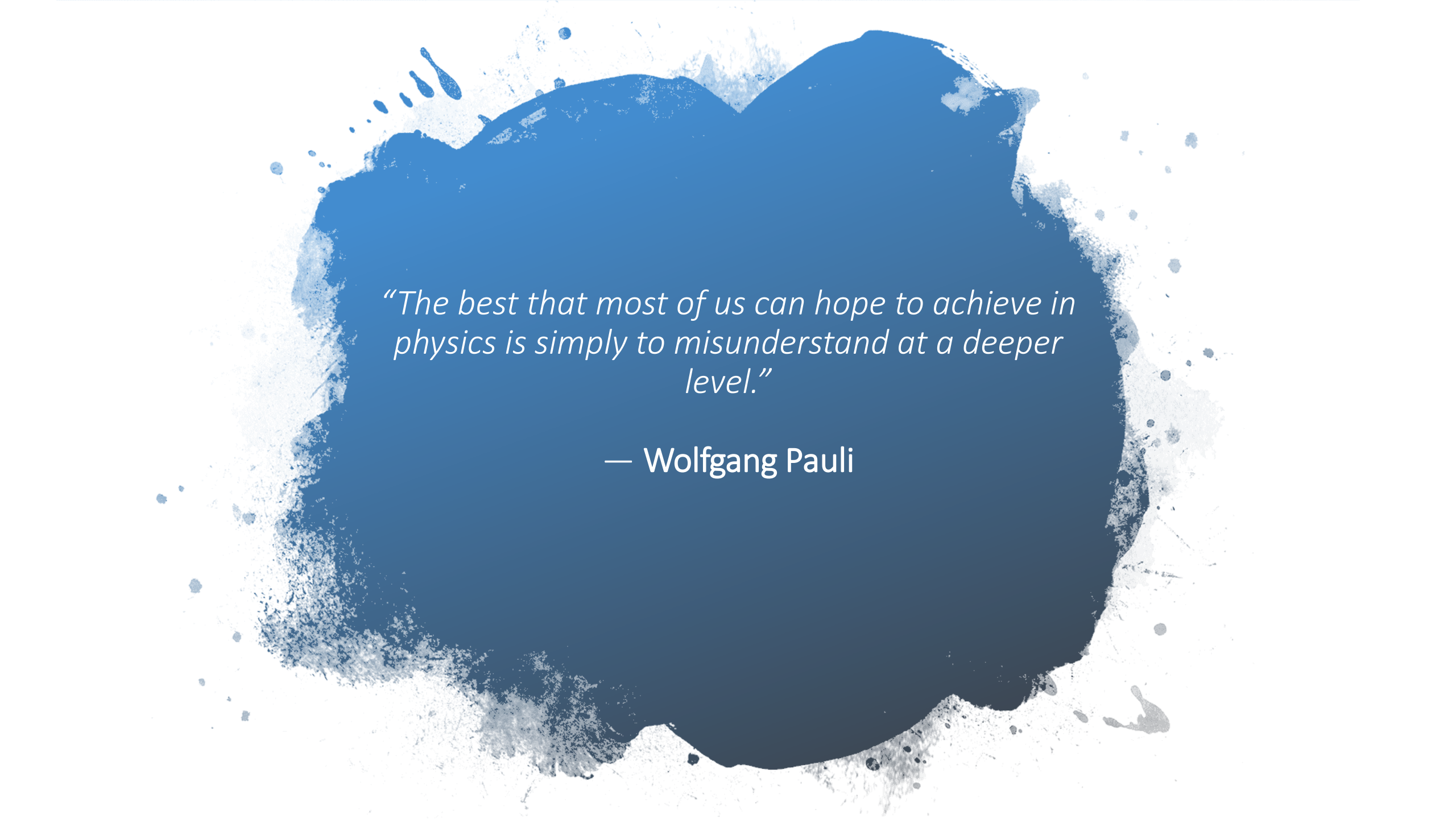


Image credit: <https://www.eag.com/>

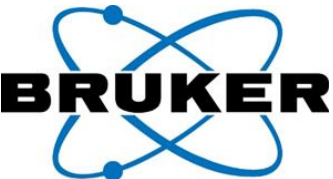


*“The best that most of us can hope to achieve in physics is simply to misunderstand at a deeper level.”*

— Wolfgang Pauli

# Thank You to Our AMC 2025 Sponsors

## Platinum sponsors:



Quantum Design



Surface Measurement System:  
World Leader in Sorption Science



Teledyne Princeton Instruments

## Sponsors:





**ILLINOIS**

Materials Research Laboratory

GRAINGER COLLEGE OF ENGINEERING